Proteomics and Glycomics Analyses of *N*-Glycosylated Structures Involved in *Toxoplasma gondii*-Host Cell Interactions*[S]

Sylvain Fauquenoy‡, Willy Morelle‡, Agnès Hovasse§, Audrey Bednarczyk§, Christian Slomianny¶, Christine Schaeffer§, Alain Van Dorsselaer§, and Stanislas Tomavo‡‖

The apicomplexan parasite *Toxoplasma gondii* recognizes, binds, and penetrates virtually any kind of mammalian cell using a repertoire of proteins released from late secretory organelles and a unique form of gliding motility (also named glideosome) that critically depends on actin filaments and myosin. How *T. gondii* glycosylated proteins mediate host-parasite interactions remains elusive. To date, only limited evidence is available concerning *N*-glycosylation in apicomplexans. Here we report comprehensive proteomics and glycomics analyses showing that several key components required for host cell-*T. gondii* interactions are *N*-glycosylated. Detailed structural characterization confirmed that *N*-glycans from *T. gondii* total protein extracts consist of oligomannosidic ($Man_{5-8}(GlcNAc)_2$) and paucimannosidic ($Man_{3-4}(GlcNAc)_2$) sugars, which are rarely present on mature eukaryotic glycoproteins. *In situ* fluorescence using concanavalin A and *Pisum sativum* agglutinin predominantly stained the entire parasite body. Visualization of *Toxoplasma* glycoproteins purified by affinity chromatography followed by detailed proteomics and glycan analyses identified components involved in gliding motility, moving junction, and other additional functions implicated in intracellular development. Importantly tunicamycin-treated parasites were considerably reduced in motility, host cell invasion, and growth. Collectively these results indicate that *N*-glycosylation probably participates in modifying key proteins that are essential for host cell invasion by *T. gondii*. *Molecular & Cellular Proteomics 7:891–910, 2008.*

Apicomplexans are protozoan parasites defined by the presence of a complex of specialized organelles at their apical end (1). The phylum Apicomplexa contains many important pathogens of humans and animals, including the causative agents of malaria (*Plasmodium* spp.) and chicken coccidiosis (*Eimeria* spp.) as well as some of the opportunistic infections associated with AIDS patients such as *Cryptosporidium parvum* and *Toxoplasma gondii*. *T. gondii* is uniquely adapted to infect a wide range of hosts, including virtually all warm blooded animals and up to 50% of the world's human population. The primary transmission route in humans is via ingestion of undercooked contaminated meat, particularly lamb, and contact with feces from infected domestic cats. The parasite causes a serious opportunistic disease (toxoplasmosis) in congenitally infected infants that can lead to severe syndromes including congenital malformations such as blindness, mental retardation, and hydrocephaly in children exposed *in utero*. More attention has been paid to *T. gondii* because toxoplasmosis is a common opportunistic infection in immunocompromised individuals with AIDS and in transplant patients (2, 3). Although the parasite has a sexual cycle occurring in cats, in mammalian non-feline hosts, *T. gondii* is found in two haploid asexual forms, the rapidly replicating tachyzoites and the slowly dividing, quiescent encysted bradyzoites. Infection during the acute phase is rapidly established in the host by the fast replicating tachyzoites, which can invade a broad range of cell types. Unlike other protozoan pathogens that hijack the pre-existing host cell uptake machinery, *T. gondii* actively gains entry into host cells. Penetration is of paramount importance for survival and relevant to its pathogenesis during acute infection. In response to immune defense, tachyzoites differentiate into encysted bradyzoites that remain in the brain and other organs throughout the life of chronically infected hosts. The reactivation of encysted bradyzoites into actively replicating and cytolytic tachyzoites is the cause of fatal toxoplasmic encephalitis in AIDS patients (4). Like all apicomplexan parasites, *T. gondii* lacks cilia or flagella throughout most of its life cycles and enters into host cells using an unusual form of gliding motility (5). The process of host cell invasion also requires contact with the host cell plasma membrane followed by reorientation and generation of a motive force ensured by the actomyosin motor, which drives gliding and penetration into a novel, parasite-induced structure called the parasitophorous vacuole (6–9). Success-

From the ‡Unité de Glycobiologie Structurale et Fonctionnelle, CNRS UMR 8576, Université des Sciences et Technologies de Lille, 59655 Villeneuve d'Ascq, France, §Laboratoire de Spectrométrie de Masse Bioorganique, CNRS UMR 7178, Université Louis Pasteur, 67087 Strasbourg, France, and ¶Laboratoire de Physiologie Cellulaire, INSERM U 800, Université des Sciences et Technologies de Lille, 59655 Villeneuve d'Ascq, France

Received, August 17, 2007, and in revised form, January 9, 2008
Published, MCP Papers in Press, January 9, 2008, DOI 10.1074/mcp.M700391-MCP200

ful invasion of host cells requires a highly regulated release of proteins from several parasite organelles, namely micronemes, rhoptries, and dense granules (Ref. 7 and see details in Fig. 9*C*). Microneme discharge occurs first. Their contents are involved in the attachment to the host cell membrane and the formation of a connection with the parasite's actomyosin system, thereby providing the motive force that drives motility and invasion (8, 9). We speculate that glycosylation of parasite proteins may be important for host cell recognition and invasion by *T. gondii*.

Protein *N*-glycosylation serves a wide variety of functions including signaling through interaction with lectins, protein stabilization, protease resistance, endosome sorting, protein folding, and secretion (10). In eukaryotes, the precursor for *N*-glycans is built up on the lipid carrier dolichol (Dol)[1] located in the endoplasmic reticulum (ER) membrane. Current evidence has established that the biosynthetic pathway is defined by the synthesis of the protein *N*-glycosylation precursor oligosaccharide $Glc_3Man_9(GlcNAc)_2$-PP-Dol. In most eukaryotes, this biosynthetic pathway of $Glc_3Man_9(GlcNAc)_2$-PP-Dol is highly conserved, and the glycan portion is transferred en bloc via the action of oligosaccharyltransferase enzymes to Asn residues within Asn-*X*-(Ser/Thr) sequons during protein translation and sequestration into the lumen of the ER (10, 11). However, it has been shown that other eukaryotes can transfer structures other than the largest lipid-linked oligosaccharide precursor, Dol-PP-$Glc_3Man_9(GlcNAc)_2$ (12–14). Processing of the precursor structure by glycosidase and glycosyltransferase enzymes within the ER and Golgi apparatus generates the final set of mature glycan structures.

Although studies have clearly highlighted *N*-glycosylation as an essential modification for protein folding, stability, half-life, secretion, and other relevant biological functions in most eukaryotic cells, very little is known concerning this issue in *T. gondii.* The presence of *N*-glycoproteins is indeed still controversial (15–19). In general, *N*-glycosylation is considered a rare post-translational modification in apicomplexan parasites. For example, the causative agent of malaria, *Plasmodium falciparum*, lacks most genes involved in lipid (dolichylpyrophosphate)-linked oligosaccharide donors (20). We applied proteomics and glycomics analyses as well as pharmacological approaches to elucidate the parasite's *N*-glycosylation biosynthetic pathway. This led to the elucidation of the major structures of protein *N*-linked glycans that suggests the presence of an almost complete early *N*-glycosylation biosynthetic pathway in *T. gondii*. In particular, we showed that several key proteins involved in gliding motility, moving junction, and other functions that are essential for host cell invasion by *T. gondii* are modified by *N*-glycosylation. Consistently inhibition of this post-translational modification dramatically impaired the parasite's motility, host cell invasion, and intracellular growth.

[1] The abbreviations used are: Dol, dolichol; ER, endoplasmic reticulum; PP, pyrophosphate; HFF, human foreskin fibroblast; DMEM, Dulbecco's modified Eagle's medium; ConA, concanavalin A; PSA, *P. sativum* agglutinin; GC, gas chromatography; SAG, surface antigen; MIC, micronemal protein; GRA, dense granule protein; ROP, rhoptry protein; PNGase, peptide-N^4-(*N*-acetyl-β-glucosaminyl)asparagine amidase; PMAA, partially methylated alditol acetate; BLAST, Basic Local Alignment Search Tool; PFA, paraformaldehyde; mAb, monoclonal antibody; Hex, hexose; HexNAc, *N*-acetylhexosamine; Tg, *T. gondii*; MyoA, myosin A; MLC, myosin light chain; GAP, gliding-associated protein; RON, rhoptry neck protein; AMA, apical membrane antigen.

EXPERIMENTAL PROCEDURES

Growth and Isolation of Parasites—Human foreskin fibroblasts (HFFs) were maintained in Dulbecco's modified Eagle's medium (DMEM, BioWhittaker, Verviers, Belgium) supplemented with 10% fetal calf serum, 2 mM glutamine (Sigma), and 0.05% gentamycin (Sigma). Tachyzoites from RH or 76K strains were grown in monolayers of HFF cells, harvested, and purified as described previously (21). Encysted bradyzoites were purified from brains of mice chronically infected by *T. gondii* 76K for 2 months (22). These *in vivo* bradyzoites were freed by pepsin digestion (0.05 mg·ml^{-1} pepsin in 170 mM NaCl, 60 mM HCl) for 5–10 min at 37 °C. For some experiments, we generated transgenic lines of *T. gondii* 76K expressing β-galactosidase using the plasmid containing the promoter 5′GRA1 and untranslated 3′SAG1 that drives β-galactosidase expression as described previously (23). This plasmid also contains TUB1-CAT-3′SAG1, which allowed the expression of chloramphenicol acetyltransferase for selection of *T. gondii* stable transgenic β-galactosidase-expressing clones. One of the β-galactosidase-expressing clones of *T. gondii* was used to quantify parasite numbers during host cell infection and growth.

Detergent Extraction of Toxoplasma Proteins, Reduction, and Carboxyamidomethylation—Proteins were extracted on ice in a buffer of 0.5% (w/v) SDS in 100 mM Tris·HCl (pH 7.4). Insoluble material was removed by centrifugation at 3000 rpm for 15 min. Detergent was removed by extensive dialysis against 50 mM ammonium bicarbonate at 4 °C. The protein extracts were dissolved in 500 μl of 600 mM Tris·HCl (pH 8.3) and denatured by guanidine hydrochloride (6 M final concentration). The sample was incubated at 45 °C for 90 min, and the number of disulfide bridges was reduced using 300 μg of DTT. The sample was flushed with argon and incubated at 45 °C for 5 h. After addition of 1.8 mg of iodoacetamide, the sample was flushed with argon and incubated at room temperature overnight in the dark. The sample was then extensively dialyzed against 50 mM ammonium bicarbonate at 4 °C and lyophilized.

Tryptic, PNGase F, PNGase A, or α-Mannosidase Digestions—The reduced carboxymethylated proteins were digested with L-1-tosylamide-2-phenylethylchloromethylketone bovine pancreas trypsin (EC 3.4.21.4; Sigma) with an enzyme-to-substrate ratio of 1:20 (by mass), and the mixture was incubated for 24 h at 37 °C in 50 mM ammonium bicarbonate. The reaction was terminated by boiling for 5 min before lyophilization.

PNGase F (peptide-N^4-(*N*-acetyl-β-glucosaminyl)asparagine amidase, EC 3.5.1.52; Roche Applied Science) digestion was carried out in ammonium bicarbonate buffer for 16 h at 37 °C. The reaction was terminated by lyophilization, and the products were purified on a Sep-Pak C_{18} (Waters Ltd.) to separate the *N*-glycans from the peptides. After conditioning the Sep-Pak C_{18} by sequential washing with methanol (5 ml) and 5% acetic acid (2 × 5 ml), the sample was loaded onto the Sep-Pak, and the glycans were eluted with 3 ml of 5% acetic acid. Peptides were eluted with 3 ml of 80% acetonitrile containing 5% acetic acid. Acetonitrile was evaporated under a stream of nitrogen, and the samples were freeze-dried. Glycopeptides remaining

after PNGase F digestion were further digested with PNGase A (peptide-N^4-(*N*-acetyl-β-glucosaminyl)asparagine amidase, EC 3.5.1.52; Roche Applied Science) in ammonium acetate buffer (50 mM, pH 5.0) for 16 h at 37 °C using 0.5 milliunit of the enzyme. The reaction was terminated by lyophilization, and the products were purified on a Sep-Pak C_{18} (Waters Ltd.) as described above.

α-Mannosidase digestion was carried out on PNGase F-released glycans using the following conditions: 0.5 unit of enzyme (jack bean α-mannosidase, EC 3.2.1.24; Sigma) in 200 μl of 50 mM ammonium acetate buffer, pH 4.5. The enzyme digestion was incubated at 37 °C for 48 h with a fresh aliquot of enzyme added after 24 h and terminated by boiling for 10 min before lyophilization. An aliquot corresponding to 25% of the total sample was taken after the digestion and permethylated for MALDI-TOF-MS and gas chromatography (GC)-MS analysis.

Permethylation of Glycans—Permethylation of the freeze-dried glycans was performed according to the procedure developed by Ciucanu and Kerek (24). The reaction was terminated by adding 1 ml of ultrapure water followed by three extractions with 500 μl of chloroform. The pooled chloroform phases (1.5 ml) were then washed eight times with ultrapure water. The methylated derivative-containing chloroform phase was finally dried under a stream of nitrogen, and the extracted products were further purified on a Sep-Pak C_{18}. The Sep-Pack C_{18} was sequentially conditioned with methanol (5 ml) and water (2 × 5 ml). The derivatized glycans dissolved in methanol were applied on the cartridge, washed with 3 × 5 ml of water and 2 ml of 10% (v/v) acetonitrile in water, and eluted with 3 ml of 80% (v/v) acetonitrile in water. Acetonitrile was evaporated under a stream of nitrogen, and the samples were freeze-dried.

MALDI-TOF-MS—MALDI-TOF-MS experiments were carried out on a Voyager Elite DE-STR Pro instrument (PerSeptive Biosystems, Framingham, MA) equipped with a pulsed nitrogen laser (337 nm) and a gridless delayed extraction ion source. The spectrometer was operated in the positive reflectron mode by delayed extraction with an accelerating voltage of 20 kV, a pulse delay time of 200 ns, and a grid voltage of 66%. All spectra shown represent accumulated spectra obtained by 400–500 laser shots. Permethylated glycans were co-crystallized with 2,5-dihydroxybenzoic acid as matrix (10 mg/ml 2,5-dihydroxybenzoic acid in methanol/water solution (50:50)). The instrument was externally calibrated with a maltose ladder encompassing the *m/z* values of the analyzed samples.

Linkage Analysis—The permethylated native *N*-glycans were hydrolyzed in 300 μl of 4 M TFA at 100 °C for 4 h. After removing TFA by drying *in vacuo*, the permethylated compounds were then reduced at room temperature overnight by adding 200 μl of 2 M ammonia solution containing sodium borodeuteride (4 mg/ml). The reduction was terminated by adding acetic acid, and borates were eliminated under a stream of nitrogen in the presence of methanol containing 5% (v/v) acetic acid. After adding 20 μl of pyridine and 200 μl of acetic anhydride, peracetylation was carried out at 100 °C for 2 h. After evaporation under a stream of nitrogen, the partially methylated alditol acetates (PMAAs) were dissolved in chloroform, and the chloroform phase was washed 10 times with water. This PMAA-containing phase was finally dried under a stream of nitrogen, and the PMAAs were dissolved in methanol before GC-MS analysis. GC separation of PMAAs was performed using a Carbo Erba GC 8000 gas chromatograph fitted with a 25-m × 0.32-mm CP-Sil5 CB low bleed capillary column, 0.25-μm film phase (Chrompack France, Les Ullis, France). The temperature of the Ross injector was 260 °C. Samples were analyzed using a temperature program starting by a gradient of 2 °C/min from 130 to 180 °C after 2 min at 130 °C followed by a gradient of 4 °C/min until 240 °C. The column was coupled to a Finnigan Automass II mass spectrometer. PMAA analyses were performed in the electron impact mode using an ionization energy of 70 eV. Quantification of the various PMAA derivatives was carried out using total ion current of the MS detector in the positive ion mode.

Affinity Chromatography Using Concanavalin A-linked Agarose—All purification steps were carried out at 4 °C. Purified tachyzoites of RH strain (10^9 parasites) were lysed with 1 ml of buffer A containing 10 mM Tris·HCl (pH 7.5), 150 mM NaCl, 1 mM $CaCl_2$, 1 mM $MnCl_2$, 1% Triton X-100, and protease inhibitor mixture (Roche Diagnostics). After 1 h at 4 °C, insoluble material was removed by centrifugation at 10,000 × *g* for 15 min. The supernatant was incubated with concanavalin A (ConA)-agarose beads (from *Canavalin ensiformis*, jack bean, Type VA, Sigma) for 3 h and washed five times with buffer A without protease inhibitors. After a final wash with 62.5 mM Tris·HCl (pH 6.8), the bound proteins were eluted with 2 volumes of 2× SDS sample buffer and boiled at 95 °C for 5 min or with 0.5 M α-methyl-D-mannoside. Competition assays were also performed using ConA beads incubated with protein extract in the presence of 0.5 M α-methyl-D-mannoside. Large scale purification of glycoproteins for proteomics analyses was also performed according to the protocol described above except that protein extracts from 10^{10} tachyzoites were used. The eluted samples were analyzed by SDS-PAGE followed by Coomassie Blue staining.

Protein Identification by Mass Spectrometry—In-gel digestion was performed with an automated protein digestion system, MassPREP station (Waters, Milford, MA). The gel plugs were washed twice with 50 μl of 25 mM NH_4HCO_3 and 50 μl of ACN. The cysteine residues were reduced by 50 μl of 10 mM DTT at 57 °C and alkylated by 50 μl of 55 mM iodoacetamide at room temperature. After dehydration of the gel bands with ACN, the proteins were digested overnight in gel with 50 μl of 12.5 ng/μl modified pig trypsin (Promega, Madison, WI) in 25 mM NH_4HCO_3 at room temperature. The peptides released were extracted twice with 60% ACN in 5% formic acid and 100% ACN followed by excess ACN removal. Tryptic digests were analyzed by nano-LC-MS/MS using an Agilent 1100 series HPLC-Chip/MS system with a 43-mm reversed phase C_{18} column (Agilent Technologies, Palo Alto, CA) coupled to an HCTultra ion trap (Bruker Daltonics, Bremen, Germany). The voltage applied to the capillary cap was optimized to −1750 V. For tandem MS experiments, the system was operated with automatic switching between MS and MS/MS modes. The three most abundant peptides and preferentially doubly charged ions were selected on each MS spectrum for further isolation and fragmentation. The MS/MS scanning was performed in the ultrascan resolution mode at a scan rate of 26.000 *m/z* per second. A total of six scans were averaged to obtain an MS/MS spectrum. The complete system was fully controlled by ChemStation (Agilent Technologies) and EsquireControl (Bruker Daltonics) softwares.

Mass data collected during nano-LC-MS/MS analysis were processed, converted into *.mgf files, and searched first against the National Center for Biotechnology Information non-redundant (NCBInr) database using a local Mascot™ server (Matrix Science, London, UK). In addition, an in-house genome database was constructed using the complete genome sequence, downloaded as a single text file from The Institute for Genomic Research, and segmented into regular segments of well chosen length (7500 bp) with a determined overlap length (2500 bp). This nucleic acid database was imported into the local Mascot server, and the segments were translated in all possible reading frames.[2] Once expressed coding regions were identified thanks to the matching peptides on the genome sequence, the protein functions were determined by MS-BLAST sequence similarity searches. Searches were also performed using the annotated genome sequence available at ToxoDB. In both cases,

[2] S. Fauquenoy, W. Morelle, A. Hovasse, A. Bednarczyk, C. Slomianny, C. Schaeffer, A. Van Dorsselaer, and S. Tomavo, unpublished data.

protein identification was validated according to the established guidelines for proteomics data publication (25–27).

N-Glycosylated Protein Identification by Mass Spectrometry—Tryptic digests were analyzed by nano-LC-MS/MS using an Agilent 1100 series HPLC-Chip/MS system with a 43-mm carbon graphite column (Agilent Technologies) coupled to an HCTplus ion trap (Bruker Daltonics). The voltage applied to the capillary cap was optimized to −1750 V. The mass spectrometer ion transmission parameters were optimized for high *m/z* (1000 *m/z*). For tandem MS experiments, the system was operated with automatic switching between MS and MS/MS modes. The three most abundant peptides and preferentially doubly charged ions were selected on each MS spectrum for further isolation and fragmentation. The MS/MS scanning was performed in the ultrascan resolution mode at a scan rate of 26.000 *m/z* per second. A total of six scans were averaged to obtain an MS/MS spectrum. The complete system was fully controlled by ChemStation (Agilent Technologies) and EsquireControl (Bruker Daltonics) softwares. For each protein identified, potential *N*-glycosylation sites were predicted using the NetNGlyc 1.0 Server, and *in silico* tryptic digestion was performed to generate the tryptic peptides containing a potential *N*-glycosylation site in their amino acid sequence. For each analysis, typical glycopeptide diagnostic ions were extracted from MS/MS ion current, and MS/MS spectra containing diagnostic ions were manually interpreted. Results were validated taking into account the following three types of fragment ions classically generated for glycopeptides: sugar neutral losses, non-glycosylated peptide fragments, and glycan backbone internal fragments.

Western Blotting—Glycoproteins, affinity-purified using a ConA column, resuspended in 2× SDS sample buffer and freshly isolated tachyzoites lysed with the same sample buffer were separated on SDS-polyacrylamide gels under non-reducing conditions and blotted to nitrocellulose by an electrophoretic transfer system (Bio-Rad system). Blots were blocked in TNT buffer (15 mM Tris·HCl (pH 8), 140 mM NaCl, 0.05% Tween 20) with 5% dry milk and incubated with primary antibodies (monoclonal or rabbit polyclonal antibodies) followed by goat anti-rabbit IgG or goat anti-mouse IgG conjugated to peroxidase (Sigma), and the signal was detected by chemiluminescence using the ECL kit (Amersham Biosciences). *T. gondii*-specific antibodies were generously provided by Drs. M. Lebrun (anti-rhoptry neck protein 2 (RON2) and anti-apical membrane antigen 1 (AMA1), D. Boothroyd (anti-AMA1), P. Bradley (anti-RON1 and anti-apicoplast), D. Soldati (anti-myosin A (MyoA), anti-MLC1, and anti-gliding-associated protein 45 (GAP45) and J.-F. Dubremetz (anti-ROP2/3/4, anti-MIC, and anti-GRA).

Lectin and Immunofluorescence Localizations—Freshly isolated and purified tachyzoites were fixed with 4% paraformaldehyde (PFA) in PBS for 30 min on ice. For the localization of glycoproteins, fixed slides were permeabilized with 0.1% Triton X-100 prepared in buffer B containing 10 mM Tris·HCl (pH 7.5), 0.15 M NaCl, 1 mM $CaCl_2$, 1 $MnCl_2$ at room temperature. Free PFA was blocked by 0.1 M glycine in buffer C (similar to buffer B except that the Triton X-100 was at 0.01%) for 10 min at room temperature. Then parasites were incubated either with 10 μg/ml biotinylated concanavalin A (Type IV, Sigma) or 100 μg/ml FITC-coupled *Pisum sativum* agglutinin (PSA; Sigma) diluted in buffer C for 30 min at 37 °C. After three washes with buffer C, the ConA-treated slides were incubated with FITC-coupled streptavidin (Sigma) for 30 min at 37 °C and washed three times. For co-localization, slides containing intracellular parasites were incubated with lectins followed by incubation with monoclonal or polyclonal antibodies in PBS with 0.01% Triton X-100. Fluorescently conjugated secondary antibodies were added and incubated for 30 min at 37 °C. After three washes, slides were mounted in ImmunO (immunofluor mounting medium, MP Biochemicals Inc.), examined, and photographed on a Zeiss confocal microscope.

In Vitro Gliding Assays—Intracellular tachyzoites of the RH strain were treated with 5 μg/ml tunicamycin (Sigma) prepared at an initial concentration of 1 mg/ml in DMSO for 40 h at 37 °C. The untreated intracellular parasites incubated in DMSO only or tunicamycin-treated parasites were filtered as described above; chased with DMEM containing 10 mM HEPES, 1 mM EGTA; and centrifuged at 1,000 rpm for 10 min at room temperature. The parasite pellet was resuspended in medium as above, and 5×10^8 tunicamycin-treated or untreated tachyzoites were inoculated into a chamber containing a slide that had previously been coated overnight with 50% fetal calf serum in PBS. The slides were then incubated with the parasites at 37 °C for 15 min, rinsed in PBS, and fixed in 4% PFA in PBS. Trails left by gliding parasites were visualized by staining with the monoclonal antibody anti-surface antigen (SAG) 1 and photographed using a Zeiss Axiophot microscope.

Parasite Attachment, Host Cell Invasion, and Growth—To test parasite attachment and invasion, two assays were used to distinguish parasites that had attached and entered host cells from those that had entered and replicated in host cells. First, freshly purified tachyzoites of RH strain treated with tunicamycin or untreated parasites as described above were resuspended in DMEM containing 10% FCS, loaded onto slides containing confluent monolayer HFF cells, incubated at 37 °C for 10 min, then fixed with 4% PFA, and processed for immunofluorescence analysis. Second, tunicamycin-treated or untreated tachyzoites of RH strain were also loaded onto confluent monolayer HFF cells for 1 h, and intracellular growth was monitored for 24 h at 37 °C. Slides were rinsed with PBS, fixed with 4% PFA, washed with PBS, and stained with mAb anti-SAG1 followed by FITC-goat anti-mouse IgG. Attached/invaded parasites for 10 min-pulse infection or 1-h infection followed by growth for 24 h were quantified by single tachyzoites or replicated tachyzoites, and counting was performed for at least 500 host cells. Experiments were repeated three times, and data are expressed as the mean ± S.D. Third, parasite growth was alternatively quantified by using freshly isolated β-galactosidase-expressing 76K strain parasites to infect slides in 24-well plates containing HFF cells for 4 h at 37 °C. Four wells were individually treated with 5 μg/ml tunicamycin or DMSO alone. After 2 days of growth, one-fifth of each well was used to infect a new well containing monolayer HFF cells, and incubation was continued for 2 days under tunicamycin or DMSO treatment. The remaining parasites of the first cycle experiment were recovered, washed with PBS, and frozen. After the second cycle of treatment, one-fifth of each well was used to infect new monolayer HFF cells for the third cycle experiment. The parasite pellets were washed with PBS and lysed with buffer containing 100 mM HEPES (pH 8.0), 1 mM $MgSO_4$, 5 mM DTT, 1% Triton X-100. The β-galactosidase activity was quantified using a chlorophenol red-β-D-galactopyranoside (Roche Applied Science) colorimetric assay (23). Three independent experiments were performed, and data are expressed as mean ± S.D.

RESULTS

MALDI-TOF-MS of N-Glycans Released from Detergent Extracts—To gain more insight into protein *N*-glycosylation by the parasite, we embarked on the determination of the major structures of *N*-glycans synthesized by *T. gondii*. Experimental strategies based on derivatization, chemical hydrolysis, exoglycosidase digestions, MALDI-TOF-MS, and GC-MS were used to characterize the glycans of *Toxoplasma* total protein extracts. Reduced and carboxamidomethylated *Toxoplasma* products were first digested with trypsin, and glycans were released from the resulting peptide/glycopeptide mixture by digestion with PNGase F. This enzyme is capable of releasing all known *N*-linked oligosaccharides except those

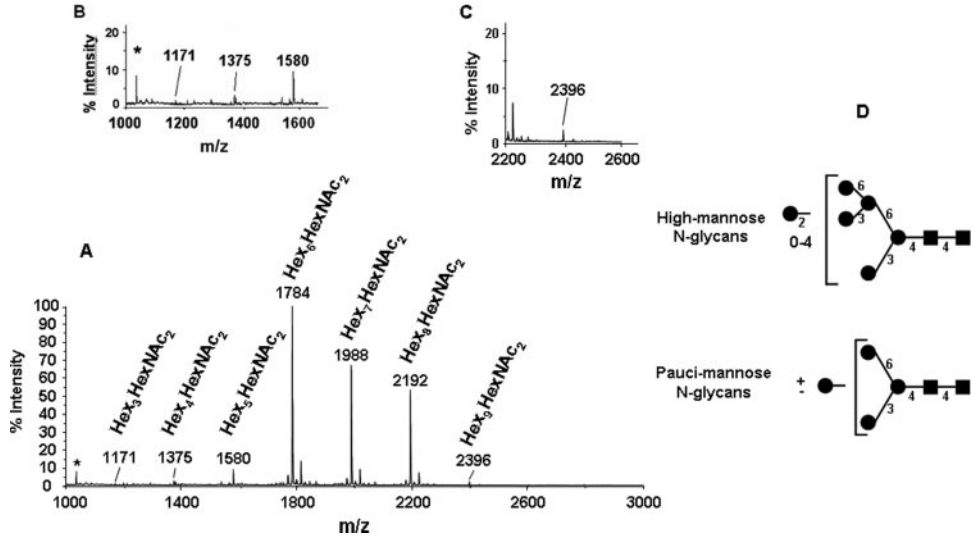

FIG. 1. **Positive MALDI-TOF mass spectrum of permethylated *N*-glycans from *T. gondii* glycoproteins.** *A*, the *N*-glycans were released from tryptic glycopeptides by digestion with PNGase F, separated from peptides by Sep-Pak purification, and permethylated. The three major molecular ions identified are $Hex_6(HexNAc)_2 + Na^+$ (*m/z* 1784), $Hex_7(HexNAc)_2 + Na^+$ (*m/z* 1988), and $Hex_8(HexNAc)_2 + Na^+$ (*m/z* 2192), which correspond to $Man_6(GlcNAc)_2$, $Man_7(GlcNAc)_2$, and $Man_8(GlcNAc)_2$, respectively. *, contaminants from the MALDI-TOF DHB solution used to resuspend the solution. *B* and *C*, four minor molecular ions, $Hex_3(HexNAc)_2 + Na^+$ (*m/z* 1171), $Hex_4(HexNAc)_2 + Na^+$ (*m/z* 1375), $Hex_5(HexNAc)_2 + Na^+$ (*m/z* 1580), and $Hex_9(HexNAc)_2 + Na^+$ (*m/z* 2396) corresponding, respectively, to $Man_3(GlcNAc)_2$, $Man_4(GlcNAc)_2$, $Man_5(GlcNAc)_2$, and $Man_9(GlcNAc)_2$ were also detected and are depicted in the *insets B* and *C* to view these minor peaks relative to the three major peaks. Ions that appear at *m/z* values slightly higher than those assigned to $Hex_{5-8}(HexNAc)_2$ in the spectrum correspond to species 30 Da larger than the fully methylated carbohydrate molecules (51). *D*, our proposed structures of *N*-glycans isolated from total extract glycoproteins of *T. gondii*. These fine *N*-glycan structures were determined twice in two independent productions of purified *T. gondii* materials by combining several enzymatic digestions, MALDI-TOF-MS, and GC-MS analyses. ■, *N*-acetylglucosamine; ●, mannose.

with fucose attached to the 3-position of the Asn-linked GlcNAc residue. Such PNGase F-resistant oligosaccharides have been found to be sensitive to PNGase A. PNGase F-released glycans were separated from peptides and were analyzed by MALDI-TOF-MS after permethylation and purification on a Sep-Pak C_{18} (Fig. 1). The permethylation derivatization of glycans increases the sensitivity of the detection of molecular ions. The peptide fraction was further digested with PNGase A, and the putative glycans released were analyzed by MALDI-TOF-MS after permethylation and purification on a Sep-Pak C_{18}. Fig. 1*A* shows the MALDI-TOF mass spectrum profile of the permethylated PNGase F-released glycans from *Toxoplasma* detergent extracts. Permethylated glycans give $[M + Na]^+$ species as the major ion. Three major molecular ions that correspond to $Hex_6(HexNAc)_2 + Na^+$ (*m/z* 1784), $Hex_7(HexNAc)_2 + Na^+$ (*m/z* 1988), and $Hex_8(HexNAc)_2 + Na^+$ (*m/z* 2192) were observed. Four minor molecular ions corresponding to $Hex_3(HexNAc)_2 + Na^+$ (*m/z* 1171), $Hex_4(HexNAc)_2 + Na^+$ (*m/z* 1375), $Hex_5(HexNAc)_2 + Na^+$ (*m/z* 1580), and $Hex_9(HexNAc)_2 + Na^+$ (*m/z* 2396) were also identified. Fig. 1, *insets B* and *C*, show enlargements of a spectrum that revealed these four minor species. Based on the MALDI-TOF-MS data and currently accepted models of *N*-glycan biosynthesis (10, 11), we conclude that the major *N*-glycans of *T. gondii* have compositions consistent with high mannose type structures ($Hex_{5-8}(HexNAc)_2$). Very minor *N*-glycans have compositions consistent with paucimannose type structures ($Hex_{3-4}(HexNAc)_2$). After PNGase F digestion, the peptide fraction was further digested with PNGase A. Putative PNGase A-released *N*-glycans were permethylated, purified on a Sep-Pak C_{18} cartridge, and analyzed by MALDI-TOF-MS. No signals corresponding to *N*-glycans were observed (data not shown). Thus, the PNGase F digestion was complete, and we could find no evidence that *N*-linked glycans with fucose attached to the 3-position of the Asn-linked GlcNAc were an important component of *Toxoplasma*. In addition, also no modification of terminal galactose and sialic acid was identified, suggesting that *T. gondii* may lack a part of the endoplasmic reticulum and Golgi trimming and maturation pathways that are highly conserved in other eukaryotes (10, 11).

Structural Analyses of N-Glycans Released by PNGase F—Linkage analyses on the PNGase F-released glycans by GC-MS shown in Table I are fully consistent with high mannose and paucimannose type structures being the constituents of the *N*-glycan population as terminal mannose and 2-linked mannose are the major residues. To define the anomeric configurations and also to confirm the presence of high mannose type structures, *N*-glycans released by PNGase F were subjected to treatment with α-mannosidase. An aliquot was taken after the digestion, permethylated, and examined by MALDI-TOF-MS after Sep-Pak C_{18} purification. After α-mannosidase treatment, the molecular ions at *m/z* 1171 ($Hex_3(HexNAc)_2$), 1375 ($Hex_4(HexNAc)_2$), 1580 ($Hex_5(HexNAc)_2$), 1784 ($Hex_6(HexNAc)_2$), 1988 ($Hex_7(HexNAc)_2$), 2192 (Hex_8-

TABLE I
GC-MS analysis of partially methylated alditol acetates obtained from the PNGase F-released N-glycans

Retention time	Characteristic fragment ions	Assignment	Relative abundance
min			
18.40	102, 118, 129, 145, 161, 162, 205	Terminal mannose	0.81
22.34	129, 130, 161, 190	2-Linked mannose	1.00
28.36	118, 129, 189, 234	3,6-Linked mannose	0.58
33.30	117, 159, 233	4-Linked GlcNAc	0.38

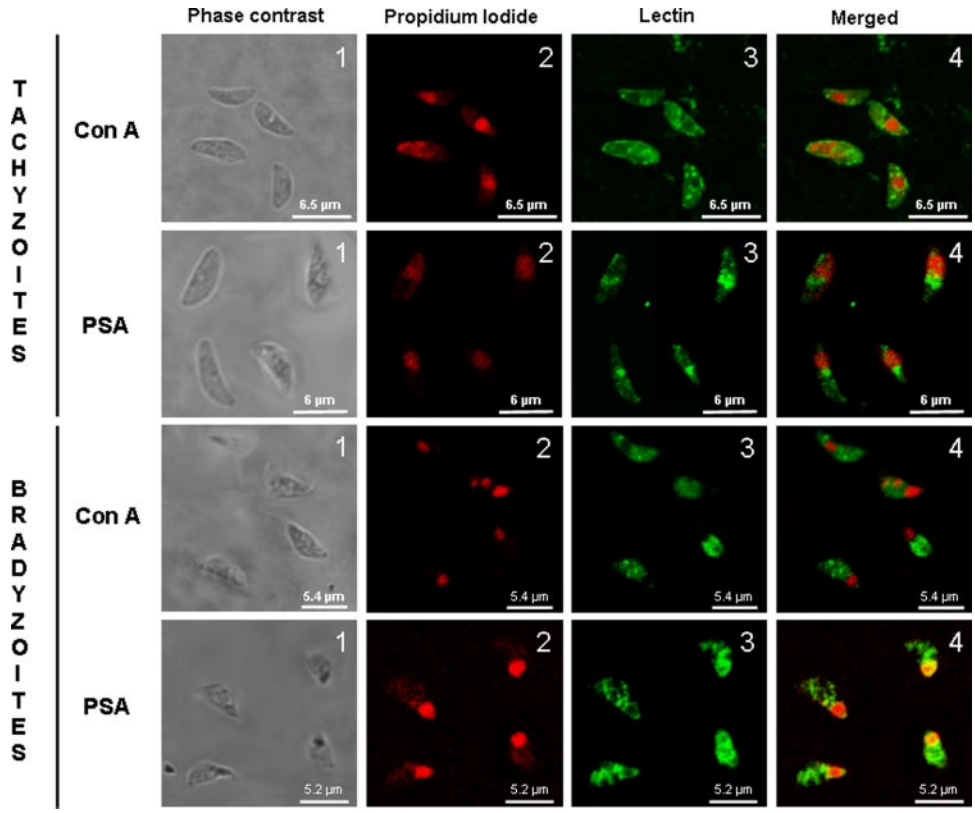

FIG. 2. **Confocal microscopy analysis of lectin-staining formaldehyde-fixed *T. gondii*.** Extracellular tachyzoites were purified from infected human foreskin fibroblasts, and bradyzoites were isolated from brains of mice chronically infected by *T. gondii*. ConA that is specific to α-D-mannose and α-D-glucose and PSA that exclusively recognizes α-D-mannose were used. The ConA signal was amplified by the FITC-conjugated streptavidin, whereas PSA was directly conjugated to FITC. *Panels 1*, phase-contrast. *Panels 2*, propidium iodide staining of nucleus (*red*). Note that mRNAs are also labeled by this dye, and the *yellow* signals around the nucleus (*panel 4*, *PSA*) indicate co-localization between the lectin signal and the endoplasmic reticulum-containing mannose-rich glycoproteins and lipid precursors and the propidium iodide staining. *Panels 3*, lectins. *Panels 4*, merged signal between propidium iodide staining and lectin labels.

$(HexNAc)_2$), and 2396 ($Hex_9(HexNAc)_2$) were abolished with a concurrent increase in signals consistent with the core of digested *N*-glycans $Hex_1(HexNAc)_2$ (*m/z* 763) and Hex_2-$(HexNAc)_2$ (*m/z* 967). Taken together, these detailed structural analyses indicated that the major *Toxoplasma N*-linked glycans are composed of high mannose ($Man_{5-8}(GlcNAc)_2$) and paucimannose ($Man_{3-4}(GlcNAc)_2$) type structures (Fig. 1*D*).

Subcellular Localization of Toxoplasma N-Glycoproteins—Indirect fluorescence staining of *T. gondii* was carried out to localize novel glycoproteins within extracellular parasites. Based on the structural data suggesting the apparent lack of complex type of *N*-glycans with sialic acid, fucose, and galactose residues in *T. gondii*, the two lectins ConA and PSA that recognize oligomannosidic glycans were tested. Although ConA is specific to both terminal α-D-mannose and α-D-glucose residues, PSA defines an exclusive terminal α-D-mannose-binding lectin. We decided to test both lectins to discriminate the signal of a polymer glucose named amylopectin that is abundantly present in the cytoplasm of bradyzoites and to a lesser extent in tachyzoites of *T. gondii* (28). When stained with ConA, the rapidly replicating tachyzoite forms that cause the acute phase of the disease (toxoplasmosis) revealed a fluorescence signal covering the entire body of the tachyzoites with a few dots of cytoplasmic punctate

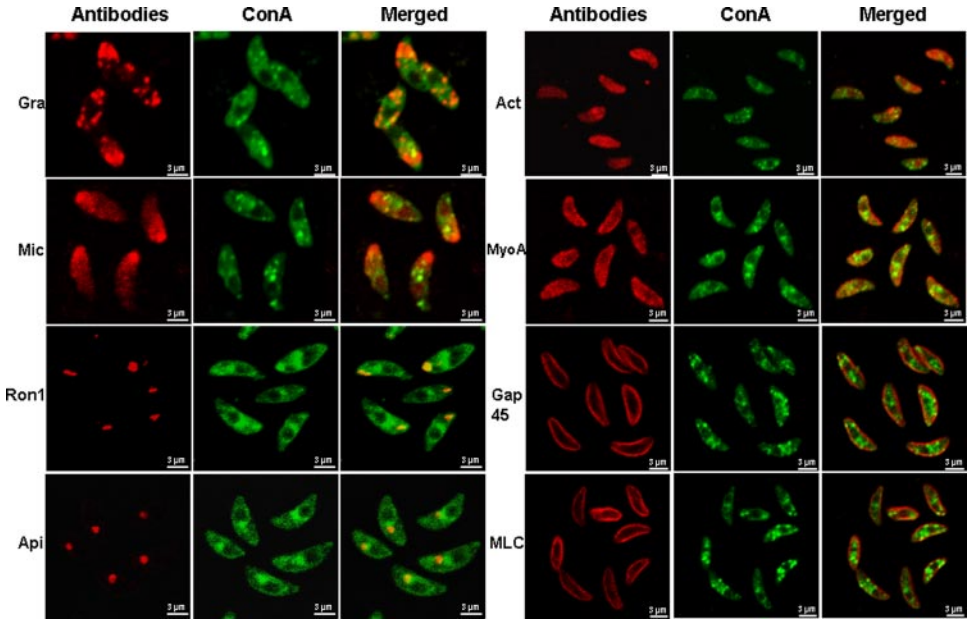

FIG. 3. **Colocalization of ConA fluorescence with different *T. gondii* organelle-specific markers.** Double fluorescence assays were performed using ConA revealed with FITC-conjugated streptavidin followed by incubation with monoclonal or polyclonal antibodies specific for protein markers of rhoptries (*Ron1*), microneme (*Mic1*), dense granules (*Gra1*), apicoplast (*Api*), actin (*Act*), MyoA, gliding-associated protein (*Gap45*), and myosin light chain 1 (*MLC*). The signals corresponding to monoclonal and polyclonal antibodies were revealed by a secondary goat Alexa Fluor 594-conjugated antibody (*red*). *Panel 1*, monoclonal or polyclonal antibody; *panel 2*, ConA; *panel 3*, merged signals between antibodies and ConA. The images were examined and photographed on a Zeiss confocal microscope.

fluorescence (Fig. 2, *panel 3*). No specific or obvious labeling of late secretory organelles could be distinctly observed (Fig. 2, *panel 3*). The lectin PSA also gave identical cytoplasmic patterns in tachyzoites (Fig. 2, *PSA*, *panel 3*) with the presence of pronounced staining of vesicles found close to the nucleus stained in red by propidium iodide (*panel 2*). We also investigated the presence of lectin-stained glycoproteins in the dormant encysted bradyzoite forms that are responsible for the chronic phase of the disease. The released bradyzoites obtained from 2-month-old cysts isolated from chronically infected mice also positively stained with both ConA and PSA, suggesting the presence of *N*-linked glycoproteins in the dormant form of *T. gondii* (Fig. 2, *Bradyzoites*, *Con A*, *panel 3*). The patterns of ConA and PSA showed clusters of scattered staining throughout the cytoplasm of bradyzoites (Fig. 2, *Bradyzoites*, *panels 3*), suggesting that these dormant parasite stages are still expressing *N*-linked glycans *de novo*. We cannot rule out that *N*-glycoproteins produced in tachyzoites or at the beginning of bradyzoite differentiation (in younger bradyzoites) are stably conserved throughout the life cycle of encysted bradyzoites. With the exception of lectin signals scattered throughout the whole body of the parasite and surrounding the nucleus (Fig. 2, *PSA*, *panel 4*, *yellow staining*) that suggest endoplasmic reticulum recognition, our experimental observations using a confocal microscope did not allow us to make a conclusion about the presence of *N*-glycoproteins in *T. gondii*-specific secretory organelles named rhoptries, micronemes, and dense granules that are known to be involved in the host cell attachment, invasion, and intracellular growth of *T. gondii.*

Colocalization of ConA Signal with Specific Markers of Subcellular Compartments of T. gondii—Indirect immunofluorescence and ConA staining of *T. gondii* tachyzoites were carried out to co-localize the lectin signal with that of several antibodies that are markers of different subcellular compartments. Fig. 3 shows diverse degrees of co-localization between ConA and markers of *T. gondii* late secretory organelles such as dense granules (mAb anti-GRA1, *Gra panel*) and micronemes (mAb anti-micronemal protein 1 (MIC1), *Mic panel*). Most importantly, a strong co-localization with *T. gondii* rhoptry neck protein 1 was revealed by a specific polyclonal antibody (*Ron1 panel*). Staining myosin A and actin with specific antibodies showed a pattern displaying weaker co-localization with ConA fluorescence (*Act* and *MyoA panels*) than that seen for RON1 (*Ron1 panel*). In addition, no convincing co-localization was observed when polyclonal antibodies specific to gliding-associated protein 45 (*Gap45 panel*) and myosin light chain (*MLC panel*), two markers of the glideosome located between the inner complex membrane and the parasite's plasma membrane, were tested. Because it has been described that one major component of the glideosome, TgGAP50 is *N*-glycosylated (19), the lack of convincing co-localization of lectin fluorescence with glideosome proteins might be explained by the weakness of the lectin signal. Alternatively the *N*-glycans carried by these proteins may be involved in protein-protein and/or glycan-protein interactions

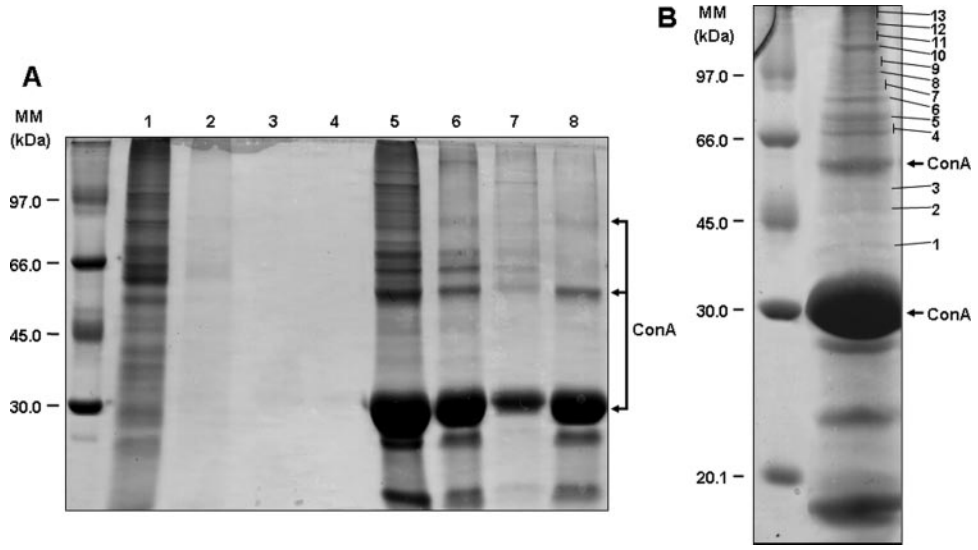

FIG. 4. **Purification of *T. gondii N*-linked glycoproteins using a ConA column.** *A*, the pilot experiment performed with detergent extract from 10^9 tachyzoites. *Lane 1*, total detergent extract used; *lanes 2–4*, efficacy of purity of glycoprotein-binding ConA column checked by taking three aliquots corresponding, respectively, to the first, third, and fifth/last washes; *lane 5*, eluate of ConA-binding glycoproteins using 2× SDS sample buffer; *lane 6*, competition assay performed by incubating the detergent protein extract in the presence of 0.5 M α-methylmannoside inhibitor before elution as described in *lane 5*; *lane 7*, elution of ConA-binding glycoproteins with 0.5 M α-methylmannoside; *lane 8*, elution of ConA beads alone by 2× SDS sample buffer. *B*, large scale purification of ConA-binding glycoproteins using detergent extract from 10^{10} tachyzoites. After elution with 2× SDS sample buffer and SDS-PAGE, 13 bands were excised and processed for proteomics analyses. The contaminated proteins corresponding to different ConA species eluted from the beads are indicated by *arrows*. *MM*, molecular mass in kilodaltons.

that may render these structures inaccessible to lectin recognition. Interestingly an apparent co-localization was observed with the apicoplast, a plastid-like organelle found in apicomplexan parasites (depicted in Fig. 9*C*) using a monoclonal antibody specific to this organelle (Fig. 3, *Api panel*). As it has been described that proteins translocated into apicoplast are transported across the endoplasmic reticulum (29), we hypothesize that some apicoplast proteins containing potential glycosylation sequons may in fact be *N*-glycosylated. This issue will be further discussed.

Nature of N-linked Glycoproteins Binding to ConA—It was difficult to firmly establish which of the parasite's specific organelles and *N*-glycoproteins were labeled by fluorescence using these lectins. Affinity purification therefore was carried out for the isolation of *N*-linked proteins that bind to ConA. A pilot experiment was performed using a total detergent extract of 10^9 tachyzoites, and the ConA-binding glycoproteins eluted were checked by SDS-PAGE followed by Coomassie Blue staining (Fig. 4*A*). After five successive washes were tested for efficiency (Fig. 4*A*, *lanes 2–4*), *N*-linked glycosylated proteins bound to ConA-beads were eluted by 2× SDS sample buffer. Interestingly only glycoproteins ranging from 45 kDa to higher than 100 kDa were identified (Fig. 4, *lane 5*). The specificity of *N*-glycosylated proteins binding to ConA was demonstrated by a competition assay performed by incubating detergent protein extracts in the presence of 0.5 M α-methylmannoside inhibitor (*lane 6*). Alternatively the elution was directly performed with the same inhibitor (*lane 7*) instead of SDS sample buffer (*lane 5*). The disappearance of numerous glycoproteins when the competition assay was performed or their appearance during the specific elution with 0.5 M α-methylmannoside suggested the presence of several *N*-glycosylated proteins ranging between 45 and >100 kDa. Then large scale preparation was performed using total detergent extract from 10^{10} tachyzoites. Thirteen gel slices (bands) were excised from the gel (as indicated in Fig. 4*B*) and digested with trypsin as described under "Experimental Procedures." The resulting peptides were analyzed by nano-LC-MS/MS, and the peak lists generated were submitted to classical protein database searches via the Mascot search engine that identified 26 proteins (proteins not footnoted in Tables II and III and supplemental data). Proteins were identified using a minimum of two matching peptides, and only unambiguous identifications with at least two matching peptides presenting high quality MS/MS spectra (MS/MS ion score higher than 40) were retained. As the predicted proteome of *T. gondii* was not fully represented and annotated in the available protein databases we decided to use a six-frame translation of the complete genome sequence in a second step for the protein identification. This approach allowed the identification of 11 additional proteins that were not present in the NCBI protein database of *T. gondii* (proteins footnoted in Table III and supplemental data). In many cases, the same protein was detected in multiple gel slices as mentioned above presumably due to carryover of high abundance proteins from one band to another during SDS-PAGE because of partial degra-

TABLE II
Proteins identified by mass spectrometry using nano LC-MS/MS analysis and the NCBInr databases

Protein name	Organism	Accession number	Molecular mass (theoretical)	Start-end	Sequences	Gel bands	Potential *N*-glycosylation sites in sequence
			Da				
MyoA (TgM-A)	*T. gondii*	gi|50400802	93,334	5–12	TTSEELKTATALK	2, 3, 6, 7, 8, 9, 10, 11, 12, 13	9 sites (67, 147, 184, 245, 246, 345, 489, 659, 672)
				35–56	GFQIWTDLAPSVKEEPDLMFAK		
				126–143	NQIYTTADPLVVAINPFR		
				144–155	DLGNTTLDWIVR		
				156–164	YRDTFDLSK		
				165–174	LAPHVFYTAR		
				176–185	ALDNLHAVNK		
				222–240	IQNAIMAANPVLEAFGNAK		
				253–260	FMQLDVGR		
				266–276	FGSVVAFLLEK		
				288–297	SYHIFYQMCK		
				307–316	FHILPLSEYK		
				317–342	YINPLCLDAPGIDDVAEFHEVCESFR		
				374–386	DGGIDDAAAIEGK		
				394–404	ACGLLFLDAER		
				413–422	VSYAGNQEIR		
				425–434	WKQEDGDMLK		
				440–455	AMYDKLFMWIIAVLNR		
				465–479	IFMGMLDIFGFEVFK		
				480–497	NNSLEQFFINITNEMLQK		
				498–509	NFVDIVFDRESK		
				520–531	ELIFTSNAEVIK		
				537–563	NNSVLAALEDQCLAPGGSDEKFLSTCK		
				577–602	VSPNINFLISHTVGDIQYNAEGFLFK		
				609–634	AEIMEIVQQSKNPVVAQLFAGIVMEK		
				676–684	KPLDWVPSK		
				685–701	MLIQLHALSVLEALQLR		
				709–719	RPFKEFLFQFK		
				756–761	TMVFLK		
				774–793	ECLSSWEPLVSVLEAYYAGR		
				803–808	TPFIIR		
				815–831	RHLVDNNVSPATVQPAF		
MyoB/C (TgM-B)	*T. gondii*	gi|50400803	132,672	132–149	SIIYTTAEPLLVAINPFK	13	B: 8 sites (83, 94, 180, 181, 304, 427, 619, 648); C: 9 sites (42, 153, 164, 250, 251, 374, 497, 689, 718)
				215–224	FFASASSEVR		
				225–245	TTIQDTIMAGNPILEAFGNAK		
				574–584	LEPSGFFLESR		
				823–836	HLEPDSINISPEER		
				1069–1080	DVSYLIGMLFQR		
Membrane skeleton protein IMC2A	*T. gondii*	gi|133990372	168,268	65–78	VLNIEVYTYLAGAK	11, 12, 13	5 sites (49, 363, 400, 409, 449)
				117–124	GLPYNVLR		
				152–159	TLNDLLLK		
				244–253	NAVETITVEK		
				261–273	LLLIGNTGIGEYK		
				288–303	FLWTNEFDQTVSALAK		
				337–343	WYDIFVK		
				347–369	LDIPWLMTLGEEEALVNPSASVR		
				475–483	LQYVDDLYK		
				555–566	GALYPILCWSGR		

TABLE II—*continued*

Protein name	Organism	Accession number	Molecular mass (theoretical)	Start-end	Sequences	Gel bands	Potential *N*-glycosylation sites in sequence
			Da				
				590–599	FFAPVNSQYK		
				620–630	DYLVAEFIDSR		
				649–660	DIQFMDPVAEGR		
				700–711	FYQTEINDLVSK		
				744–760	IAQAVSEMNVLAGDYDK		
				767–782	ELIDLKDTMPAADDPR		
				783–791	YAQLFQLEK		
				826–834	MILNMQVIR		
				836–845	EIVAVENDIK		
				933–944	GTQEELAAMQQR		
				957–963	VWQLLQR		
				976–989	ILVNQVEKLPEETR		
				1041–1054	AELVLAQESLLSEK		
				1158–1168	VSPLLSPEER		
				1174–1185	LVGPVQDLPQKK		
Actin	*T. gondii*	gi|1703160	41,908	30–40	AVFPSIVGKPK	2, 3, 6, 8, 9, 11, 12	1 site (13)
				97–114	VAPEEHPVLLTEAPLNPK		
				149–178	TTGIVLDSGDGVSHTVPIY-EGYALPHAIMR		
				185–192	DLTEYMMK		
				198–211	GYGFTTSAEKEIVR		
				240–255	SYELPDGNIITVGNER		
				256–270	FRCPEALFQPSFLGK		
				317–327	ELTSLAPSTMK		
				361–373	EEYDESGPSIVHR		
Tubulin β chain (β-tubulin)	*T. gondii*	gi|135499	49,814	63–77	AILMDLEPGTMDSVR	13	2 sites (184, 370)
				78–103	AGPFGQLFRPDNFVFGQT-GAGNNWAK		
				163–174	IMETFSVFPSPK		
				253–262	LAVNLIPFPR		
				283–297	ALSVPELTQQMFDAK		
Membrane anchor for myosin XIV precursor	*T. gondii*	gi|46948064	46,607	54–68	FVGLGNWGSGSYGQK	1, 3	3 sites (101, 136, 228)
				105–121	WQSEFENVYSDANGALK		
				122–135	MPFFTVLGVDDWSR		
				144–156	TELTYAVTSEQIKDGK		
				160–178	LAPADATEAAAAENHGYPK		
				240–246	TLELAPK		
				247–257	ILDYIIVVADR		
				267–280	GDSMLQYYLQPLLK		
				322–347	HSGSLYYAGETGFCLFELTA-EGLVTR		

dation during sample preparation or because of the presence of multiple protein isoforms due to heterogeneity of *N*-linked glycans carried by these proteins. Where a protein was detected in multiple gel slices (column designated Gel bands) and multiple MS data sets were obtained, all the matching peptides identified are shown (column designated Sequences). The nature of *T. gondii* proteins identified during this proteomics study is in good agreement with the molecular masses in kilodaltons of proteins that specifically bind to the ConA as determined by SDS-PAGE (Fig. 4). Further experimental verification of proteomics data using Western blot analyses also validated the presence of different proteins such as myosin A, GAP45, and rhoptry proteins in the *T. gondii* material eluted by affinity purification using ConA beads (data not shown). The three surface proteins including the minor glycosylphosphatidylinositol-anchored surface glycoprotein gp23, which has been described previously as an *N*-linked glycosylated protein (17), were not detected in the ConA-binding glycoproteins (data not shown). This suggests that either lower amounts of gp23 or its particular *N*-glycan modifications might explain the absence of gp23 identification. These results also confirm the absence of co-localization between the ConA signal and the major surface antigen SAG1 using a specific monoclonal antibody (data not shown). Several proteins of dense granules and micronemes tested by Western blots using specific monoclonal antibodies were also

TABLE III
Identification of additional ConA binding proteins by mass spectrometry

Protein name	Organism	Accession number	Molecular mass (theoretical)	Start - end	Sequences	Gel bands	Potential *N*-glycosylation sites in sequence
			Da				
Rhoptry neck protein 2	*T. gondii*	gi|71559160	155,451	248–259 507–520 616–629 995–1010	VAMIDAVPSGIR VVADPTAYGEIFER TFCAQPTSFLSSFR VPGFDTISAANEQLR	11	5 sites (275, 354, 393, 844, 1340)
Rhoptry neck protein 1	*T. gondii*	gi|71559158	127,355	900–914 1096–1107	DACVNQGYQSVSLTK GTLSSQQQAFMK	7	10 sites (69, 114, 632, 720, 738, 756, 774, 792, 810, 875)
Rhoptry protein 18	*T. gondii*	gi|84618297	62,342	241–250 423–432	FVSVTTGETR LFLGDFGTYR	3	1 site (377)
Rhoptry protein 7	*T. gondii*	gi|84618158	63,414	175–197 303–313 326–343 370–389 441–455 459–466 523–531 532–544	ERPQPVFTEGDPPDLETNSL-YYR- HQALAIGLFQK FLAPFDLVTIPGKPLVQK FVEELYELPTEDRPLADAAR VVAENAQGFSPPEVR GGLLFGPR LINPSVEAR LLALQATETPEYR	2, 3, 4, 5, 6, 7, 11, 12	1 site (525)
Apical membrane antigen 1 homolog	*T. gondii*	gi|2293476	59,978	84–94 108–121 122–142 143–153 166–172 185–194 197–211 218–231 232–257 276–293 342–355 412–425	EPAGLCPIWGK NNFLEDVPTEKEYK QSGNPLPGGFNLNFVTPSG-QR ISPFPMELLEK CAEFAFK YRYPFVYDSK LCHILYVSMQLMEGK GEPPDLTWYCFKPR KSVTENHHLIYGSAYVGENP-DAFISK CLDYTELTDTVIERVESK NYGFYYVDTTGEGK FPDSFGACDVQACK	6	2 sites (58, 393)
Perforin-like protein 1	*T. gondii*	gi|118500931	124,646	423–435 448–458 797–813 1074–1088	QAVPQESVADLNR AAAPLSAVYTK AVGLTPQDLSALTGVTR TVNEPAMHVATDVGK	8	7 sites (246, 253, 333, 539, 607, 744, 1103)
Sortilin, putative[a]	*P. falciparum* (isolate 3D7)	gi|124809739	102,270		SWTEITDLLK SSEAATGTVAVDSIIVSPVDKR LVADYVVQFSWGDKK LGNTDHIFFTQHR NVDLMYTPDFGATITR QTVSLLVSTDGGK LPVEIEER YSLSLPNNIR TSTGECEFDKVLSLEGVYLAN-FK GGVWSYLK DGGVSWIEAHK LAPPRFDEDNVELL FLLSNGYFFVAK	10	8 sites (56, 112, 116, 123, 375, 869, 876, 881)
DNAJ domain protein[a]	*Plasmodium berghei*	gi|68072203	44,189		QNLYSVLGVK FKEISFAYEILNNAEK QVYDEYGEEGLER LNVSLEQLYK	2	1 site (44)

TABLE III—*continued*

Protein name	Organism	Accession number	Molecular mass (theoretical)	Start - end	Sequences	Gel bands	Potential *N*-glycosylation sites in sequence
			Da				
PfSec61[a]	*P. falciparum*	gi|3057044	52,228		VITQQMGPGFIVQNQIQDDT-CVDQGK LGHEPGDLVLVIQELPHKR IGDDLEMSIR ISLLEALVGFER SFIHLDNTPVR FMVSYPAALDEK SADPFYWMR GQQGSYPIK	2	2 sites (139, 241)

[a] These proteins were identified by our in-house constructed genome database generated using complete genome sequence, downloaded as a single text file from the TIGR and segmented into regular segments of 7500 bps with a determined overlap length of 2500 bps. These nucleic acid databases were imported into the local Mascot server, and the segments were translated in all possible six reading frames. The other proteins were identified as described in Table II.

not detected in the ConA-binding material (data not shown). Taken together, these data are consistent with the presence of a limited number of surface proteins, dense granules, and micronemes in the ConA-binding material analyzed by proteomics approaches. Nevertheless many novel potentially *N*-glycosylated proteins in *T. gondii* were identified.

Proteomics Analysis Reveals Many Constituents for Parasite Motility and Host-Parasite Interactions—The proteomics approaches resulted in the unexpected identification of proteins involved in gliding motility such as myosin A (30), membrane anchor myosin XIV (also named GAP50) (19), actin, and the membrane skeleton protein IMC2A. These components play key roles in the particular gliding motility of parasites that allows *T. gondii* to enter into host cells (31–33). Strikingly bioinformatics analyses indicated that these components of the glideosome contain between one and nine Asn-*X*-(Ser/Thr) sequons required for *N*-glycosylation (Table II). The second class of *N*-linked glycosylated proteins that we identified are components of the late apical secretory organelles, named rhoptries (Table III). These Asn-*X*-(Ser/Thr)-containing glycoproteins include RON2 and AMA1 involved in moving junction formation that is required for host cell invasion (34–36). RON1 contains 10 Asn-*X*-(Ser/Thr) sequons, the highest number of consensus sites identified during this study, whereas RON2 has only five consensus sites (Table III). Another category of secreted proteins present in the rhoptry was also identified (Table III and supplemental data). These are known to be released from the rhoptry during host cell invasion and participate in the formation of the vacuole in which the parasites multiply (37–39). These ROPs that bound to ConA include the protein kinase-related family members ROP2, ROP5, ROP7, and ROP18 (Table III and supplemental data). However, only ROP7 and ROP18 appeared to contain one genuine *N*-glycosylation sequon (Table III), suggesting that the other ROPs (ROP2, ROP4, and ROP5) are unlikely to be glycosylated but were pulled down together with other *T. gondii* ConA-binding *N*-linked glycoproteins. In addition, other proteins identified by proteomics also include myosin B/C known to be involved in parasite division (40) and the skeleton component tubulin (41) (Table II). Additional bioinformatics searches using our in-house genome database (see details under "Experimental Procedures") identified all potentially *N*-linked glycoproteins, and in addition to the putative partners described above, 11 novel proteins were detected (proteins marked by asterisk in Table III and supplemental data). Some of these novel putative *N*-glycoproteins are highly conserved in the Apicomplexa, implying that they fulfill parallel roles in the biology of these parasites. For example, we identified the *Plasmodium* homologue of perforin-like protein 1 (Ref. 42 and Table III) and a putative sortilin (Ref. 43 and Table III). Surprisingly HSP70, HSP90, elongation factor 1a, and eukaryotic translation initiation factor 4A were also detected (supplemental data). Finally some proteins that do not contain the Asn-*X*-(Ser/Thr) sequons were also found, confirming that unglycosylated partners can be co-precipitated with *T. gondii N*-glycoproteins (supplemental data). However, HSP70 and HSP90 may be involved in the folding and stabilization of genuine *N*-linked glycoproteins of the glideosome, moving junction, or other subcellular compartments of the parasites.

Deciphering the Precise Nature of N-Glycopeptides by Structural Analysis of Both N-Glycans and Peptides—We established the structures of *N*-linked glycopeptides of a major *T. gondii* glycoprotein, GAP50, identified by proteomics analysis by determining the nature of both *N*-linked glycans and trypsin-generated peptides. Two MS/MS spectra show the presence of typical diagnostic ions, MH^+ *m/z* 366.14 and 528.19 corresponding to glycan backbone internal fragments. Both are found in bands 1 and 3 (MS/MS spectra of doubly protonated parent ions at *m/z* 1248.10 and 1329.50). The MS/MS spectrum of the doubly protonated parent ion at *m/z* 1248.10 shows fragment ions, which correspond to sugar neutral losses on the glycopeptide. Therefore, one ion of mass MH^+ *m/z* 953.47 was observed, corresponding to the peptide

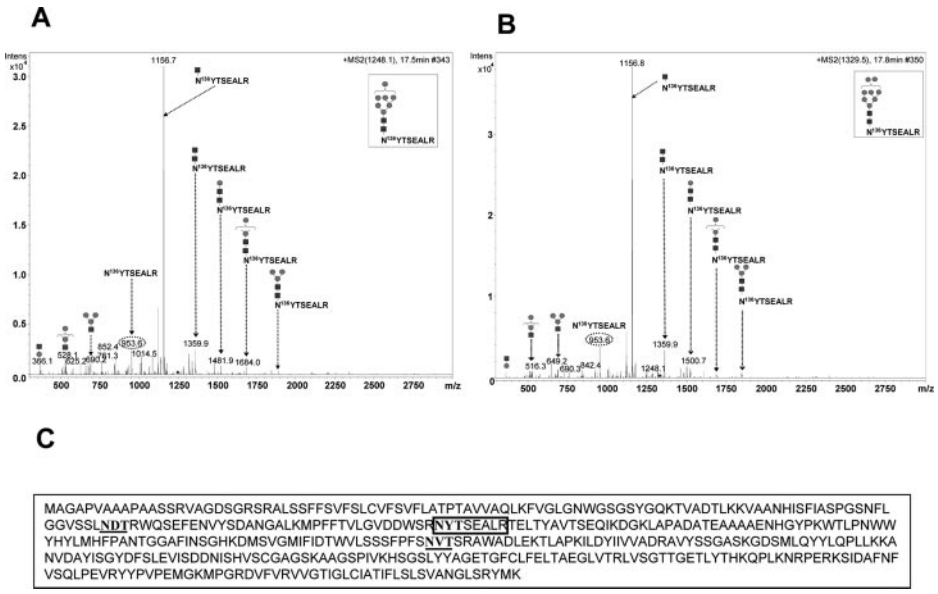

FIG. 5. **Identification of peptide and *N*-glycans from the membrane anchor myosin XIV also named GAP50.** *A*, the MS/MS spectrum from parent ion at $m/z = 1248.10$ corresponding to the peptide NYTSEALR with the *N*-glycosylation $Man_7(GlcNAc)_2$ in position Asn^{136}. *B*, the MS/MS spectrum from parent ion at $m/z = 1329.50$ corresponding to the peptide NYTSEALR with the glycosylation $Man_8(GlcNAc)_2$ in position Asn^{136}. *C*, the position of the peptide NYTSEALR with the consensus NYT alternatively modified by $Man_7(GlcNAc)_2$ and $Man_8(GlcNAc)_2$ is indicated (*boxed*) in the GAP50 protein sequence. The two additional *N*-glycosylation sequons are *underlined* and *bold*.

NYTSEALR that is a potential glycosylated tryptic peptide from the membrane anchor myosin XIV (GAP50), and was only identified in these two bands (Fig. 5). Combining the two data above allowed us to determine the glycan structure $Man_7(GlcNAc)_2$ at position Asn^{136} of GAP50 (Fig. 5*A*). In addition, the MS/MS spectrum of the doubly protonated parent ion at *m/z* 1329.50 is clearly similar to the MS/MS spectrum of parent ion *m/z* 1248.10 (same fragment ions and presence of the ion of mass MH^+ *m/z* 953.47). Only the doubly protonated parent ion masses show a mass difference of 162 Da corresponding to the mass of a mannose. These two data allowed us to define the glycan structure $Man_8(GlcNAc)_2$ at the same position, Asn^{136}, of the membrane anchor myosin XIV (GAP50) (Fig. 5*B*). Taken together, the data confirmed the presence of the following two high mannose structures, $Man_7(GlcNAc)_2$ or $Man_8(GlcNAc)_2$, on the peptide NYTSEALR with NYT as a consensus site in the membrane anchor myosin XIV. As mentioned, TgGAP50 is an integral membrane protein that anchors *T. gondii* myosin A (TgMyoA), its associated light chain (TgMLC1), actin, and TgGAP45 to the inner membrane complex, and these constitute the glideosome that is involved in motility required for host cell invasion (19). TgGAP50, which contains three Asn-*X*-(Ser/Thr) consensus sites (Fig. 5*C*, *underlined* and *bold*), has been reported previously as a genuine *N*-linked glycoprotein that can be cleaved off by PNGase F, and its mobility shift compared with PNGase F-untreated control suggested that the three consensus sites are likely occupied by *N*-glycans (19). We demonstrate here that the NYT sequon within the NYTSEALR peptide (*boxed* in TgGAP50 protein sequence in Fig. 5*C*) bears alternatively $Man_8(GlcNAc)_2$ and $Man_7(GlcNAc)_2$. The glycoprotein TgGAP50 represents a genuine pellicle component involved in the parasite's motile apparatus. However, the implication of *N*-glycosylation, not only in gliding motility but also in the biogenesis of the parasite's late secretory organelles, was further investigated in greater detail using both cell biology and pharmacological approaches.

The N-Glycosylation Inhibitor Tunicamycin Blocks T. gondii Growth within Mammalian Cells—The *N*-glycosylation inhibitor tunicamycin displayed an unexpected and intriguing mode of action on the intracellular tachyzoites of *T. gondii*. When parasite numbers were determined by a quantitative assay using the exogenous reporter enzyme β-galactosidase expressed by stable tachyzoites harboring the *lac*Z gene, we were surprised that 5 μg/ml or higher concentration of tunicamycin showed no significant inhibitory effect on the intracellular growth of *T. gondii* tachyzoites during the first round of drug treatment (Fig. 6*A*, *1st Cycle*). Instead the tunicamycin-treated tachyzoites displayed a normal replication rate until infected host cells were lysed at 48 h postinfection like the control tachyzoites treated with DMSO alone (Fig. 6*A*, *1st Cycle*). In sharp contrast, when the first round of treated tachyzoites were used to infect new host cells in the presence or absence of tunicamycin, only a 25–30% growth rate relative to untreated tachyzoites was observed, suggesting that parasites were now significantly altered in division rate during the second cycle of infection (Fig. 6*A*, *2nd Cycle*). A more drastic effect, up to 90% growth rate inhibition, was observed during the third cycle of host infection (Fig. 6*A*, *3rd Cycle*). As mentioned, the presence of tunicamycin was not required to

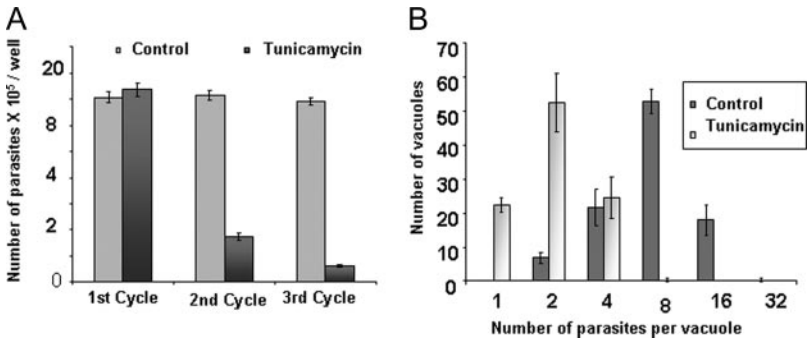

FIG. 6. **Inhibitory effect of tunicamycin on *T. gondii* growth.** *A*, the delayed effect of tunicamycin on *T. gondii* tachyzoites growth quantified using stable β-galactosidase-expressing 76K strain parasites. Four wells of 24-well plates containing HFF cells infected by tachyzoites were treated with 5 μg/ml tunicamycin or with DMSO alone. After 2 days of infection, one-fifth of each well of the first cycle treated or untreated parasites was used to infect new wells under tunicamycin or DMSO treatment. The remaining parasites of this first cycle experiment were recovered, washed with PBS, and frozen. After the second cycle of treatment, one-fifth of each well was used again to infect new monolayer HFF cells for the third cycle experiment. All parasite pellets were lysed and tested for β-galactosidase activity. Three independent experiments were performed, and data are expressed as mean ± S.D. *B*, comparison of the growth rate of tunicamycin-treated and untreated tachyzoites. Tachyzoites treated with tunicamycin or with DMSO alone during the first cycle of infection as described were loaded onto new monolayer of HFF cells and grown for 24 h in the absence of drug. The percent distribution of vacuole size (number of parasites per vacuole) was counted for 100 vacuoles in three independent experiments, and data are expressed as mean ± S.D.

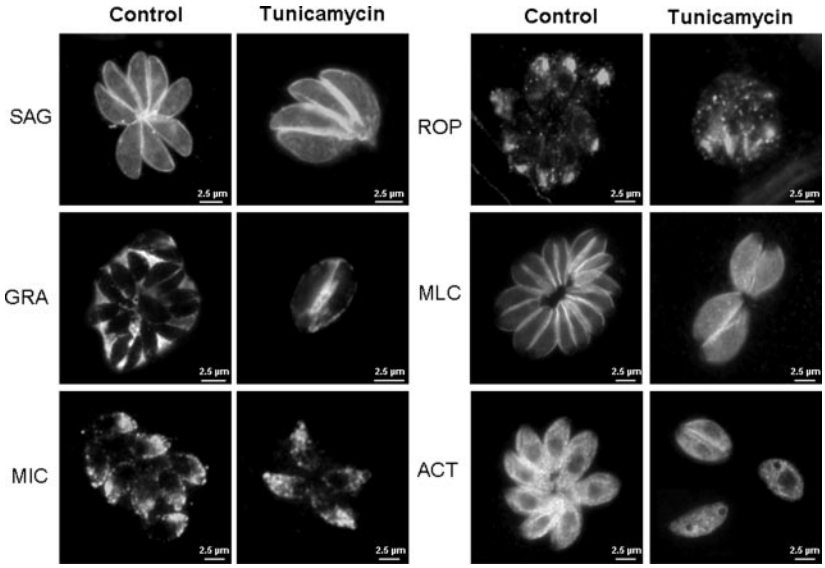

FIG. 7. **Tunicamycin alters the morphogenesis of *T. gondii* organelles.** Tachyzoites treated with tunicamycin or with DMSO alone for 48 h during the first cycle of infection were released and loaded on new monolayer HFF cells and grown for 24 h without drug. The morphology of different organelles verified by markers such as the monoclonal antibody anti-surface protein SAG1, anti-dense granule protein GRA1, anti-MIC1, anti-rhoptries ROP2/3/4, anti-MLC, and anti-actin (*ACT*) were compared between tunicamycin-treated and the control DMSO-treated *T. gondii* tachyzoites. Note the pronounced effect of tunicamycin on the morphogenesis of inner membrane complex.

obtain the significant effect on intracellular growth of the parasites during the second and third cycles. Because *T. gondii* divides by a unique binary division and because the number of parasites per vacuole reflects division rates, we examined the intracellular growth of tachyzoites after the first round of tunicamycin treatment. As can be seen in Fig. 6*B*, tachyzoites treated once with tunicamycin displayed a slower multiplication rate in their newly infected host cells. The control tachyzoites treated during the first cycle of infection with DMSO multiplied at normal rates, and 4–16 parasites/vacuole were obtained at 24 h postinfection (Fig. 6*B*). By comparison, first round tunicamycin-treated tachyzoites that received no further treatment during the second round of new host cell infection still grew more slowly. Values of one and four parasites/vacuole at 24 h post-infection were scored (Fig. 6*B*). This reduced multiplication rate that led to 1–4 parasites/vacuole in tunicamycin-treated tachyzoites *versus* untreated controls (8–16 parasites/vacuole) was also confirmed by direct visualization using immunofluorescence assays and different monoclonal antibodies (Fig. 7).

Tunicamycin Alters Biogenesis of Late Secretory Organelles and the Inner Membrane Complex—To determine whether tunicamycin could alter the morphogenesis of different secretory organelles and other subcellular compartments of *T. gondii*, tachyzoites, drug-treated for 48 h, were used to infect new monolayer HFF cells and grown for 24 h without drug. The morphology of different organelles was checked and compared with the control tachyzoites treated with DMSO and

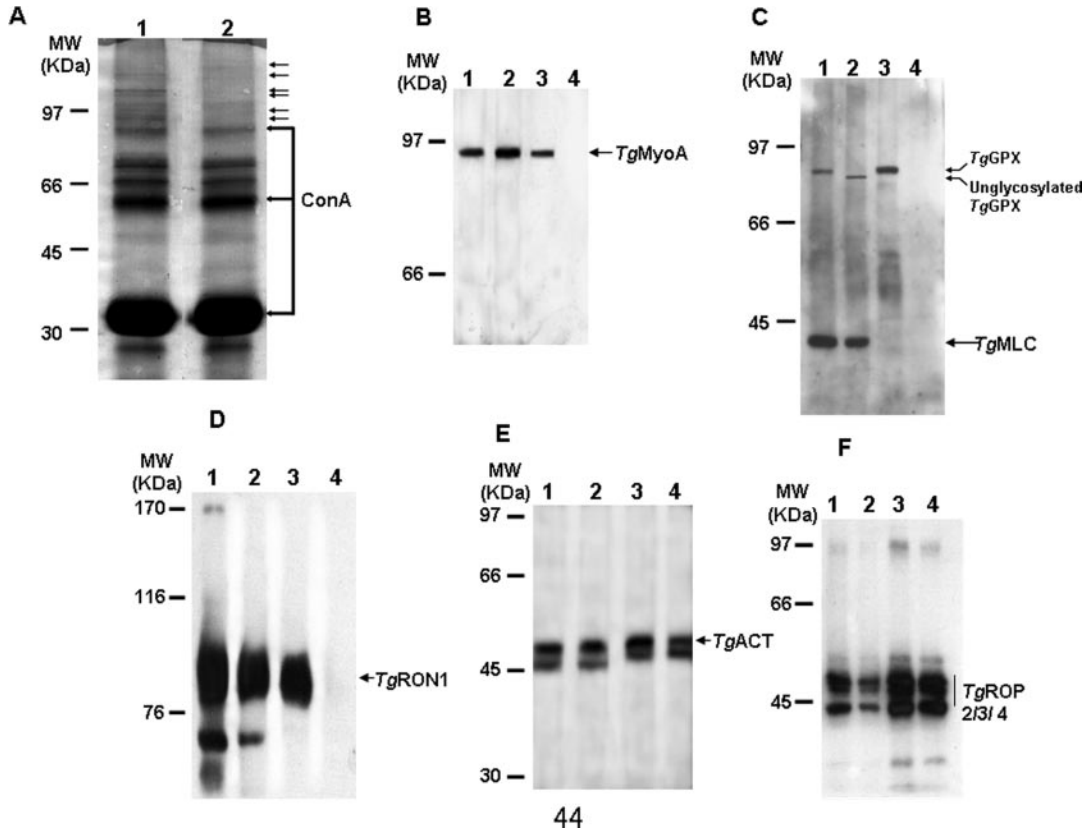

FIG. 8. **Effect of tunicamycin on ConA binding and identification of novel *N*-glycoproteins of *T. gondii.*** *A*, total detergent extract from the same number of tunicamycin-treated or untreated control (DMSO only) tachyzoites was incubated with ConA beads. After elution, the samples were analyzed by SDS-PAGE (7.5% polyacrylamide gel) followed by Coomassie Blue staining. The absence of glycoprotein binding to ConA is indicated by *arrows*. *B–F*, further verification of the tunicamycin effect on ConA binding by TgMyoA (*B*), TgMLC (*C*), TgRON1 (*D*), actin (*TgACT*; *E*), and TgROP2/3/4 (*F*) using lectin purification followed by Western blots. *Lane 1*, total detergent extract from the control tachyzoites; *lane 2*, total detergent extract from tunicamycin-treated tachyzoites; *lane 3*, presence of the parasite protein from the control tachyzoites detected in the ConA-binding material; *lane 4*, absence or presence of parasite protein from the material eluted from ConA beads when a lysate of tunicamycin-treated tachyzoites was used. Note the identification of a novel *N*-glycoprotein (*TgGPX*) that cross-reacted to anti-TgMLC antibodies. This TgGPX displayed an electrophoretic shift when the total lysate was prepared from tunicamycin-treated tachyzoites (*C*, *lane 3*) and could not bind to ConA (*C*, *lane 4*) confirming that TgGPX is *N*-glycosylated. The nature of this novel *N*-glycoprotein remains to be determined.

processed under the same experimental conditions. The plasma membrane appeared not to be affected in tunicamycin-treated tachyzoites (Fig. 7, *SAG panel*). Neither the constitutive secretion of dense granules within the vacuole nor the morphology of micronemes was affected in tunicamycin-treated tachyzoites (Fig. 7, *GRA* and *MIC panels*). In addition, the fluorescence pattern of rhoptries was not significantly changed after tunicamycin treatment (Fig. 7, *ROP panel*). In contrast, the classical fluorescence pattern of the inner membrane complex could not be visualized, suggesting that the morphogenesis of this compartment had been altered (Fig. 7, *MLC panel*). A more diffuse cytoplasmic staining was detected with anti-myosin, and the inner membrane complex that is known to be labeled by this myosin marker could not be distinguished (Fig. 7, *MLC panel*). Some treated tachyzoites also showed a few unknown structures when anti-actin was tested (Fig. 7, *ACT panel*). Collectively these data indicate that tunicamycin induces important alterations in the biogenesis of *T. gondii* inner membrane complex, suggesting that the function of the parasite's motile apparatus or glideosome that is located in this compartment may be impaired.

Inhibition of T. gondii N-Glycosylation by Tunicamycin—At the molecular level, we also demonstrated that binding of *T. gondii* glycoproteins to ConA was affected when protein extracts were derived from tunicamycin-treated tachyzoites prior to lectin affinity purification. As shown in Fig. 8*A*, several *N*-glycosylated proteins ranging from 45 to >100 kDa that specifically bound to ConA, as reported in Fig. 4*A*, were no longer detected (see Fig. 8*A*, *small arrows*). Western blots in Fig. 8*B* further validated the absence of TgMyoA from the tunicamycin-treated material eluted from ConA (*lane 4*). The polyclonal antibodies specific to myosin light chain (MLC) cross-reacted with a novel *T. gondii* glycoprotein of 85 kDa that displayed a difference in electrophoretic mobility be-

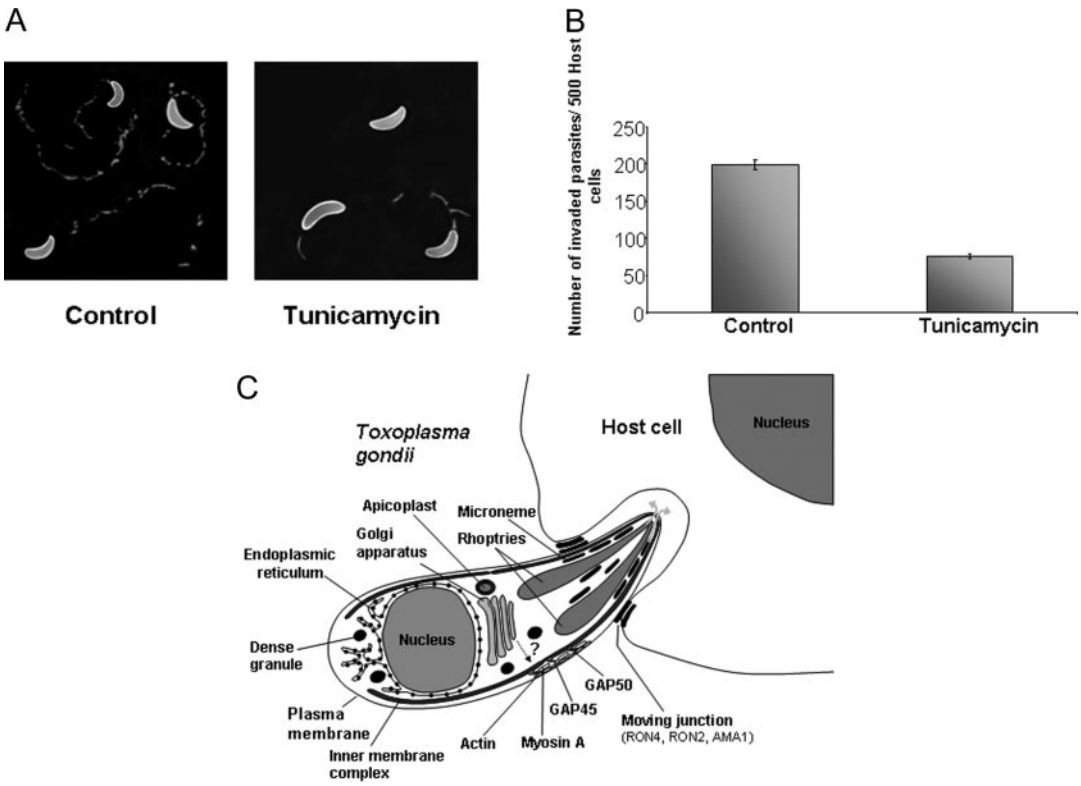

FIG. 9. **Effect of tunicamycin on *T. gondii* gliding motility and host cell invasion.** *A*, effect of tunicamycin on gliding motility of *T. gondii*. Tachyzoites treated with tunicamycin or with DMSO alone (*Control*) for 48 h during the first cycle of infection were released and allowed to glide on serum-coated slides. Trails were visualized by staining with anti-SAG1 antibodies followed by a fluorescent secondary antibody. *B*, effect of tunicamycin on host cell entry. The tunicamycin-treated and untreated tachyzoites during the first cycle of infection described above were also used to infect new monolayer HFF cells and grown for 24 h. The intracellular tachyzoites were paraformaldehyde-fixed and stained with anti-SAG1 or anti-GRA1 antibodies. 500 vacuoles were counted, and three different experiments were performed. The data are expressed as mean ± S.D. *C*, schematic drawing illustrating the host cell entry by *T. gondii*, the basic elements (ER, Golgi apparatus, and plasma membrane), and parasite-specific organelles (dense granules, micronemes, rhoptries, and apicoplast). The current accepted model of host cell entry or invasion proposes contributions from both the glideosome and the moving junction. The glideosome is composed of TgMyoA, actin filaments, and membrane anchor myosin XIV or GAP50 and GAP45, which are located between the plasma membrane and the inner membrane complex, whereas the moving junction contains rhoptry proteins that are secreted during host cell entry. These moving junction proteins include RON2, RON4, and the microneme AMA1. In light of the observations related in this study, we describe that several components of both glideosome and moving junction are potentially *N*-glycosylated or contain a number of consensus sites suggesting them to be *N*-glycosylated. We believe that this post-translational modification may be required for their proper intracellular transport to the pellicle and for protein-protein interactions.

tween tunicamycin-treated and untreated tachyzoites, respectively (Fig. 8*C*, *lanes 1* and *2*). As expected, when deglycosylated the 85-kDa protein was unable to bind ConA (*lane 4*). The precise nature of this novel 85-kDa glycoprotein remains to be determined. In addition, we demonstrated that the rhoptry neck protein RON1 was not capable of binding ConA when tunicamycin-treated (*lane 4*) compared with untreated lysate (*lane 3*). Because of the lower amount of rhoptry neck protein 2 detected by Western blots combined with our identification of only one peptide isolated by proteomics approaches, it was not surprising that we were unable to validate the *N*-glycosylated status of RON2 using total extract of tunicamycin-treated extracts (data not shown). In contrast, we were able to show that actin (Fig. 8*E*), ROP2/3/4 (Fig. 8*F*), and probably other cytoplasmic proteins can bind to ConA despite tunicamycin treatment, suggesting that these abundant proteins interact nonspecifically with the lectin. Nevertheless our proteomics data together with the direct evidence of the *N*-glycan structures $Man_7(GlcNAc)_2$ and $Man_8(GlcNAc)_2$ at position Asn^{136} of the peptide NYTSEALR of GAP50 and the lack of ConA binding by TgMyoA after tunicamycin treatment also suggest that several crucial proteins involved in the parasite's motility and host-parasite interactions are likely *N*-glycosylated.

Tunicamycin Blocks T. gondii Motility and Host Cell Invasion—To investigate the physiological role of *N*-glycosylation in the parasite's motility, we monitored the gliding of drug-treated and untreated tachyzoites using immunofluorescence staining to detect the trails left on slides by motile parasites (Fig. 9*A*). When intracellular tachyzoites were treated with 5 μg/ml tunicamycin for 40 h and purified, the freshly released and tunicamycin-treated tachyzoites were unable to display parasite-specific gliding as no characteristic trail motility was

visualized for individual parasites stuck to serum-coated glass (Fig. 9*A*, *Tunicamycin panel*). Only a few tachyzoites treated by tunicamycin showed smaller and aborted trails, whereas the untreated tachyzoites (incubated with DMSO only) that were analyzed under the same experimental conditions were entirely motile as demonstrated by the prominent trail length for each individual tachyzoite (Fig. 9*A*, *Control panel*). These data on the inhibition of *N*-glycosylation of components involved in parasite's gliding motility are consistent with tunicamycin treatment affecting the host cell invasion by *T. gondii.*

To establish whether tunicamycin was blocking the attachment or invasion of host cells, we monitored host cell reinfection after the first cycle of intracellular parasite treatment. To do this, we examined and quantified the number of parasites attached to or invading host cells. Invasion was scored during a 1-h pulse infection followed by 24 h of intracellular growth. Fig. 9*B* shows an approximately 70% decrease in tachyzoite numbers within host cells, suggesting that tunicamycin treatment impaired host cell invasion.

DISCUSSION

In this study, we have provided new evidence that *T. gondii* contains numerous *N*-glycosylated proteins that unexpectedly are components of the glideosome, moving junction, and other glycoproteins involved in host cell-parasite interactions. The cell wall or pellicle of apicomplexan parasites like *T. gondii* consists of the plasma membrane and the closely associated, flattened cisternae of the inner membrane complex. Both actin and myosin A homologues have been localized to the space between the plasma membrane and the inner membrane, and this glideosome is a key player in motility and host cell entry by *T. gondii* (see schematic model in Fig. 9*C*). Another essential element represents the moving junction, a structure built at the interface between the host cell and the parasite during its active entry into any kind of mammalian cell. The moving junction is a circumferential zone that forms at the apical tip of the parasite, moves backward, and pinches the vacuole from the host cell membrane (34, 36). Several components of the moving junction are secreted from late secretory organelles such as rhoptries (RON2) and micronemes (AMA1) (depicted in Fig. 9*C*). It is clear that the results presented here identified *N*-linked glycosylation on several key constituents involved in host-parasite interactions. The major *Toxoplasma N*-linked glycans released from total detergent extract proteins by PNGase F are oligomannosidic ($Man_{5-8}(GlcNAc)_2$) and paucimannosidic structures ($Man_{3-4}(GlcNAc)_2$), sugars that are rarely present on mature *N*-glycoproteins of higher eukaryotes. The three major *N*-glycans linked to proteins correspond to $Man_6(GlcNAc)_2$, $Man_7(GlcNAc)_2$, and $Man_8(GlcNAc)_2$, respectively. In addition, four other minor oligosaccharides, $Man_3(GlcNAc)_2$, $Man_4(GlcNAc)_2$, $Man_5(GlcNAc)_2$, and an extremely limited amount of $Man_9(GlcNAc)_2$, were also found. It has been shown that other eukaryotes can transfer structures other than the largest lipid-linked oligosaccharide precursor, Dol-PP-$Glc_3Man_9(GlcNAc)_2$ (12–14, 20). Thus, we postulate that the paucimannosidic *N*-linked glycan structures found on *T. gondii* glycoproteins could point to the transfer of $Man_5(GlcNAc)_2$ and its subsequent glucosylation as reported previously in *Trypanosoma brucei* (14). The genes encoding numerous endoplasmic reticulum-located glycosyltransferases, named *ALG* (asparagine-linked glycosylation), required for the biosynthesis of the lipid (dolichylpyrophosphate)-linked glycosyl donors and oligosaccharyltransferases needed for the *N*-glycan transfer to proteins, can be readily identified in the *T. gondii* genome (ToxoDB) using detailed bioinformatics and gene predictions.[3] All of these genes involved in both synthesis of lipid precursor and transfer of *N*-glycan structures are transcribed in *T. gondii* tachyzoites and bradyzoites.[4] In contrast, our biochemical analyses failed to detect sialylated, galactosyl, or fucosylated structures consistent with either the likely absence or the limited presence of complex glycan types containing sialic acid, galactose, and fucose residues in *T. gondii*. This also indicates that a part of the endoplasmic reticulum and Golgi trimming and maturation pathways that are highly conserved in other eukaryotes is absent in the parasite. However, only structures of major *N*-glycans were determined when the total detergent glycoprotein extracts were analyzed. We therefore cannot rule out the presence of other minor modifications and branching monosaccharides that escaped detection in this study.

We identified a number of known proteins that have not been suspected until now to be *N*-glycosylated. Conversely *N*-glycosylation is considered as a rare post-translational modification in apicomplexan parasites because most investigations have focused attention on surface and other antigens that are important for host cell-parasite interactions and future vaccine development. Our data confirmed that the key glideosome membrane anchor myosin XIV (also named GAP50), known to be involved in both parasite motility and host cell entry, contains *N*-glycosylated structures. From the mixed glycopeptide populations, we were fortunate to identify the trypsin-generated peptide NYTSRALR of the membrane anchor myosin XIV (GAP50) that is truly modified by two *N*-glycan structures at the same position, Asn^{136}. We report for the first time in *T. gondii* the fine *N*-glycan structures that are present on the GAP50 sequon NYT that is alternatively modified by $Man_8(GlcNAc)_2$ or $Man_7(GlcNAc)_2$. However, it was somewhat unexpected to find that TgMyoA, another component of the glideosome, was also capable of specifically binding to ConA. We have shown that TgMyoA failed to bind to ConA when the parasites were treated with the *N*-glycosylation poison tunicamycin. Neither the N-terminal signal peptide nor a transmembrane domain is present in TgMyoA.

[3] F. Dzierszinski, D. Ross, and S. Tomavo, unpublished data.
[4] S. Fauquenoy and S. Tomavo, unpublished data.

These data therefore suggest that an *N*-glycosylated binding partner might bring TgMyoA into interaction with ConA. As stated, no obvious domains of TgMyoA presently explain how it might be translocated across the ER membrane to the lumen where the addition of *N*-glycans is expected to occur co-translationally (10). However, almost nothing is known about ER translocation machinery in *T. gondii*, and previous work on *Saccharomyces cerevisiae* has described that carboxypeptidase Y and an acid phosphatase can be translocated to the ER, enter the secretory pathway, and be *N*-glycosylated without having their N-terminal signal sequences (44, 45). In addition, it has been shown that cytoplasmic and nuclear proteins are *N*-glycosylated, suggesting the existence of post-translational *N*-glycosylation mechanisms in higher eukaryotes (46, 47). It remains to be determined whether such a non-conventional *N*-glycosylated biosynthetic pathway operates in *T. gondii*. To our knowledge, almost nothing has been reported on *N*-glycosylation of myosins and components involved in the motile apparatus in other eukaryotic cells. Gliding is a unique form of apicomplexan parasite motility that manifests as either circular spirals or a series of helical turns revolving around the long axis of the body of the parasite (30–32). It has been suggested previously that the soluble protoglideosome and membrane-associated TgGAP50 are transported separately and are assembled into the glideosome in the inner membrane complex of mature parasites (19). The *N*-linked glycosylation of glideosome components such as GAP50 suggests that this post-translational modification may be involved in their intracellular trafficking mechanisms or in their transport to the parasite's space where the glideosome are assembled. It is also interesting to note that two key components of the moving junction (RON2 and AMA1) required for host cell invasion (Fig. 9*C*) are also present in material purified by ConA. These moving junction proteins also contain putative *N*-glycosylation sites. In addition, we showed that another rhoptry neck protein, RON1, with presently unknown function may be *N*-glycosylated. It should be mentioned that RON1 displayed the strongest fluorescence that co-localized with the ConA signal, and its deglycosylation by tunicamycin prevented lectin binding. However, we cannot rule out that RON1 may indirectly bind to ConA via other *N*-glycan-bearing RONs. We were not able to confirm that RON2 and AMA1 are *N*-glycosylated using Western blots because of the limited amount of protein detected after lectin purification. Their glycopeptides modified by *N*-glycan structures were also not identified using MALDI-MS/MS analyses because only a few peptides (only one peptide from RON2) from these proteins were obtained. Further biochemical analyses including purification of higher amounts of RON2 and AMA1 by affinity purification with their respective specific antibodies followed by direct determination of *N*-glycan structures using mass spectrometry are required. Many other proteins have been isolated by ConA affinity purification and identified by proteomics analyses. Among these are also proteins that do not have any predicted *N*-glycosylation sites (supplemental data), suggesting that these proteins may interact with other genuine *N*-glycosylated proteins. This may be the case for MIC1 (supplemental data) that has been reported previously as a parasite lectin (48) that might be retained on ConA by interacting with *N*-glycan structures carried by other *N*-glycoproteins that specifically bind to ConA. Even if some proteins without *N*-glycosylated sites (supplemental data) may behave like MIC1, we cannot exclude that these components may also interact with ConA nonspecifically as further demonstrated during this study for actin and other rhoptry proteins such as ROP2/3/4.

It is intriguing that unlike all other eukaryotic cells, *T. gondii* tachyzoites treated with tunicamycin at conventional inhibitory concentrations did not display any obvious growth defect within its host cells during its first cycle of intracellular development that lasts 48 h. The growth defect appeared only during the second cycle of reinvasion of host cells with a very prominent effect during the third cycle. The effect of tunicamycin took place in the absence of drug during the second and third cycle of host cell infection, suggesting that this delayed effect, or unusual kinetics of tunicamycin on *T. gondii*, may reflect drastic differences in host cell re-entry by tunicamycin-treated relative to untreated tachyzoites. This conclusion is supported by the results that demonstrate the ability of tunicamycin to affect gliding motility of tachyzoites released after intracellular drug treatment. We cannot exclude that host cell attachment may also be affected by tunicamycin treatment. However, the lack of *N*-glycosylation of several SAGs and most MICs reported by lectin purification and proteomics analyses indicates that any interference of host cell attachment by tunicamycin may be marginal. Therefore, we suspect that it is the parasite's motility and new host cell invasion that are likely impaired in tunicamycin-treated tachyzoites. It remains to be determined whether moving junction formation is also inhibited by tunicamycin and absence of *N*-glycosylation. However, the delayed effect on intracellular replication of tunicamycin-treated parasites that have entered new host cells is highly reminiscent of the delayed death phenomenon seen with apicoplast inhibitors (49). It appears that ConA fluorescence co-localizes with the signal of apicoplast-specific monoclonal antibodies. Because it has been described that some apicoplast proteins transit through the ER (29, 50), it is likely that this plastid-like organelle may also contain *N*-glycosylated proteins and that the delayed effects seen with tunicamycin might be partially attributable to inhibition of apicoplast functions.

In summary, the current study illuminates a diverse repertoire of *N*-glycosylated proteins that contribute to parasite survival and pathogenesis during mammalian host cell infection. Novel parasite-specific *N*-glycoproteins identified here can significantly expand the number of potential targets for therapeutic intervention. We anticipate that ongoing in-depth exploration of biological functions of the identified *N*-linked

glycans carried by components involved in gliding motility, moving junction, protein secretion, and protein-protein interaction would further unravel the invasive and pathogenic mechanisms developed by *T. gondii* and other apicomplexan parasites during infection.

Acknowledgments—We thank Drs. Dominique Soldati, Maryse Lebrun, Jean-François Dubremetz, Peter Bradley, and John Boothroyd for generous gifts of antibodies and Drs. Steven Ball and Gordon Langsley for a critical review of the manuscript. We acknowledge the *Toxoplasma* Genome Sequencing Consortium for making available the genome database. Preliminary genomic and/or cDNA sequence data were accessible via ToxoDB. The mass spectrometry facility used at the University of Lille was funded by the European Community (FEDER), the Région Nord-Pas de Calais (France), the CNRS, and the Université des Sciences et Technologies de Lille.

* This work was supported by the CNRS and INSERM. The costs of publication of this article were defrayed in part by the payment of page charges. This article must therefore be hereby marked "*advertisement*" in accordance with 18 U.S.C. Section 1734 solely to indicate this fact.

S The on-line version of this article (available at http://www.mcponline.org) contains supplemental material.

‖ To whom correspondence should be addressed: Equipe de Parasitologie Moléculaire, Unité de Glycobiologie Structurale et Fonctionnelle, CNRS UMR 8576, Bâtiment C9, Université des Sciences et Technologies de Lille, 59655 Villeneuve d'Ascq, France. Tel.: 33-3-20-43-69-41; Fax: 33-3-20-33-65-55; E-mail: Stan.Tomavo@univ-lille1.fr.

REFERENCES

1. Kim, K., and Weiss, L. M. (2004) Toxoplasma gondii: the model apicomplexan. *Int. J. Parasitol.* **34,** 423–432
2. Dubey, J. P. (1994) Toxoplasmosis. *J. Am. Vet. Med. Assoc.* **205,** 1593–1598
3. Dubey, J. P. (1998) Advances in the life cycle of *Toxoplasma gondii. Int. J. Parasitol.* **28,** 1019–1024
4. Luft, B. J., Hafner, R., Korzun, A. H., Leport, C., Antoniskis, D., Bosler, E. M., Bourland, D. D., Uttamchandani, R., Fuhrer, J., Jacobson, J., Morlat, P., Vilde, J.-L., and Remington, J. S. (1993) Toxoplasmic encephalitis in patients with the acquired immunodeficiency syndrome. Members of the ACTG 077p/ANRS 009 study team. *N. Engl. J. Med.* **329,** 995–1000
5. Dobrowolski, J. M., Carruthers, V. B., and Sibley, L. D. (1997) Participation of myosin in gliding motility and host cell invasion by *Toxoplasma gondii. Mol. Microbiol.* **26,** 163–173
6. Carruthers, V., and Boothroyd, J. C. (2006) Pulling together: integrated model of *Toxoplasma* cell invasion. *Curr. Opin. Microbiol.* **10,** 83–89
7. Carruthers, V., and Sibley, L. D. (1997) Sequential protein secretion from three distinct organelles of *Toxoplasma gondii* accompanies invasion of human fibroblasts. *Eur. J. Cell Biol.* **73,** 114–123
8. Jewett, T. J., and Sibley, L. D. (2003) Aldolase forms a bridge between cell surface adhesins and the actin cytoskeleton in apicomplexan parasites. *Mol. Cell* **11,** 885–894
9. Soldati, D., and Meissner, M. (2004) Toxoplasma as a novel system for motility. *Curr. Opin. Cell Biol.* **16,** 32–40
10. Kornfeld, R., and Kornfeld, S. (1985) Assembly of asparagine-linked oligosaccharides. *Annu. Rev. Biochem.* **54,** 631–664
11. Aebi, M., and Hennet, T. (2001) Congenital disorders of glycosylation: genetic model systems lead the way. *Trends Cell Biol.* **11,** 136–141
12. Turco, S. J., and Pickard, J. L. (1982) Altered G-protein glycosylation in vesicular stomatitis virus-infected glucose-deprived baby hamster kidney cells. *J. Biol. Chem.* **257,** 8674–8679
13. Parodi, A. J. (1993) N-Glycosylation in trypanosomatid protozoa. *Glycobiology* **3,** 193–199
14. Jones, D. C., Mehlert, A., Güther, L. S., and Ferguson, M. A. J. (2005) Deletion of the glucosidase II gene in *Trypanosoma brucei* reveals novel N-glycosylation mechanisms in the biosynthesis of variant surface glycoprotein. *J. Biol. Chem.* **280,** 35929–35942
15. Handman, E., Goding, J. W., and Remington, J. S. (1980) Detection and characterization of membrane of *Toxoplasma gondii. J. Immunol.* **124,** 2578–2583
16. de Carvalho, L., Souto-Padron, T., and de Souza, W. (1991) Localization of lectin-binding sites and sugar-binding proteins in tachyzoites of *Toxoplasma gondii. J. Parasitol.* **77,** 156–161
17. Odenthal-Schnittler, M., Tomavo, S., Becker, D., Dubremetz, J.-F., and Schwarz, R. T. (1993) Evidence for N-linked glycosylation in *Toxoplasma gondii. Biochem. J.* **291,** 713–721
18. Shans-Eldin, H., Blaschke, T., Anhlan, D., Niehus, S., Müller, J., Azzouz, N., and Schwarz, R. T. (2005) High-level expression of the *Toxoplasma gondii* STT3 gene is required for suppression of the yeast STT3 gene mutation. *Mol. Biochem. Parasitol.* **143,** 6–11
19. Gaskins, E., Gilk, S., DeVore, N., Mann, T., Ward, G., and Beckers, C. (2004) Identification of the membrane receptor of a class XIV myosin in *Toxoplasma gondii. J. Cell Biol.* **165,** 383–393
20. Samuelson, J., Banerjee, S., Magnelli, P., Cui, J., Kelleher, D. J., Gilmore, R., and Robbins, P. W. (2005) The diversity of dolichol-linked precursors to Asn-linked glycans likely results from secondary loss of sets of glycosyltransferases. *Proc. Natl. Acad. Sci. U. S. A.* **102,** 1548–1553
21. Dzierszinski, F., Popescu, O., Toursel, C., Slomianny, C., Yahiaoui, B., and Tomavo, S. (1999) The protozoan parasite *Toxoplasma gondii* expresses two functional plant-like glycolytic enzymes. Implications for evolutionary origin of apicomplexans. *J. Biol. Chem.* **274,** 24888–24895
22. Dzierszinski, F., Mortuaire, M., Dendouga, N., Popescu, O., and Tomavo, S. (2001) Differential expression of two plant-like enolases with distinct enzymatic and antigenic properties during stage conversion of the protozoan parasite *Toxoplasma gondii. J. Mol. Biol.* **309,** 1017–1027
23. Seeber, F., and Boothroyd, J. C. (1996) *Escherichia coli* β-galactosidase as an *in vitro* and *in vivo* reporter enzyme and stable transfection marker in the intracellular protozoan parasite *Toxoplasma gondii. Gene* (*Amst.*) **169,** 39–45
24. Ciucanu, I., and Kerek, F. (1984) A simple and rapid method for the permethylation of carbohydrates. *Carbohydr. Res.* **131,** 209–217
25. Carr, S., Aebersold, R., Baldwin, M., Burlingame, A., Clauser, K., and Nesvizhskii, A. (2004) The need for guidelines in publication of peptide and protein identification data. Working Group on Publication Guidelines for Peptide and Protein Identification Data. *Mol. Cell. Proteomics* **3,** 531–533
26. Bradshaw, R. A. (2005) Revised draft guidelines for proteomic data publication. *Mol. Cell. Proteomics* **4,** 1223–1225
27. Wilkins, M. R., Appel, R. D., Van Eyk, J. E., Chung, M. C., Gorg, A., Hecker, M., Huber, L. A., Langen, H., Link, A. J., Paik, Y. K., Patterson, S. D., Pennington, S. R., Rabilloud, T., Simpson, R. J., Weiss, W., and Dunn, M. J. (2006) Guidelines for the next 10 years of proteomics. *Proteomics* **6,** 4–8
28. Coppin, A., Varré, J.-S., Lienard, L., Dauvillée, D., Guérardel, Y., Soyer-Gobillard, M.-O., Buléon, A., Ball S., and Tomavo, S. (2005) Evolution of plant-like crystalline storage polysaccharide in the protozoan parasite *Toxoplasma gondii* argues for a red alga ancestry. *J. Mol. Evol.* **60,** 257–267
29. Waller, R. F., Keeling, P. J., Donald, R. G., Striepen, B., Handman, E., Lang-Unnasch, N., Cowman, A. F., Besra, G. S., Roos, D. S., and McFadden, G. I. (1998) Nuclear-encoded proteins target to the plastid in *Toxoplasma gondii* and *Plasmodium falciparum. Proc. Natl. Acad. Sci. U. S. A.* **95,** 12352–12357
30. Meissner, M., Schluter, D., and Soldati, D. (2002) Role of *Toxoplasma gondii* myosin A in powering parasite gliding and host cell invasion. *Science* **298,** 837–840
31. Dobrowolski, J. M., and Sibley, L. D. (1996) *Toxoplasma* invasion of mammalian cells is powered by the actin cytoskeleton of the parasite. *Cell* **84,** 933–939
32. Keeley, A., and Soldati, D. (2004) The glideosome: a molecular machine powering motility and host-cell invasion by Apicomplexa. *Trends Cell Biol.* **14,** 528–532
33. Sibley, L. D. (2004) Intracellular parasite invasion strategies. *Science* **304,** 248–253
34. Alexander, D. L., Mital, J., Ward, G. E., Bradley, P., and Boothroyd, J. C. (2005) Identification of the moving junction complex of *Toxoplasma*

gondii: a collaboration between distinct secretory organelles. *PLoS Pathog.* **1,** e17
35. Bradley, P. J., Ward, C., Cheng, S. J., Alexander, D. L., Coller, S., Coombs, G. H., Dunn, J. D., Ferguson, D. J., Sanderson, S. J., Wastling, J. M., and Boothroyd, J. C. (2005) Proteomic analysis of rhoptry organelles reveals many novel constituents for host-parasite interactions in *Toxoplasma gondii. J. Biol. Chem.* **280,** 34245–34258
36. Lebrun, M., Michelin, A., El Hajj, H., Poncet, J., Bradley, P. J., Vial, H., and Dubremetz, J.-F. (2005) The rhoptry neck protein RON4 re-localizes at the moving junction during *Toxoplasma gondii* invasion. *Cell. Microbiol.* **7,** 1823–1833
37. El Hajj, H., Demey, E., Poncet, J., Lebrun, M., Wu B., Galeotti, N., Fourmeaux, M. N., Mercereau-Puijalon, O., Vial, H., Labesse, G., Dubremetz, J.-F. (2006) The ROP2 family of *Toxoplasma gondii* rhoptry proteins: proteomic and genomic characterization and molecular modeling. *Proteomics* **6,** 5773–5784
38. El Hajj, H., Lebrun, M., Fourmaux, M. N., Vial, H., and Dubremetz, J.-F. (2007) Inverted topology of the *Toxoplasma gondii* ROP5 rhoptry protein provides new insights into the association of the ROP2 protein family with the parasitophorous vacuole membrane. *Cell. Microbiol.* **9,** 54–64
39. Saeij, J. P., Boyle, J. P., Coller, S., Taylor, S., Sibley, L. D., Brooke-Powell, E. T., Ajioka, J. W., and Boothroyd, J. C. (2006) Polymorphic secreted kinases are key virulence factors in toxoplasmosis. *Science* **314,** 1780–1783
40. Delbac, F., Sänger, A., Neuhaus, E., Stratmann, R., Ajioka, W. J., Toursel, C., Herm-Götz, A., Tomavo, S., Soldati, T., and Soldati, D. (2001) Toxoplasma gondii myosins B/C: one gene, two tails, two localizations, and a role in parasite division. *J. Cell Biol.* **155,** 613–623
41. Morrissette, N. S., Murray, J. M., and Roos, D. S. (1997) Subpellicular microtubules associate with an intramembranous particle lattice in the protozoan parasite *Toxoplasma gondii. J. Cell Sci.* **110,** 35–42
42. Kadota, K., Ishino, T., Matsuyama, T., Chinzei, Y., and Yuda, M. (2004) Essential role of membrane-attack protein in malarial transmission to mosquito host. *Proc. Natl. Acad. Sci. U. S. A.* **101,** 16310–16315
43. Nielsen, M. S., Madsen, P., Christensen, E. I., Nykjaer, A., Gliemann, J., Kasper, D., Pohlmann, R., and Peterson, C. M. (2001) The sortilin cytoplasmic tail conveys Golgi-endosome transport and binds the VHS domain of the GGA2 sorting protein. *EMBO J.* **20,** 2180–2190
44. Blachy-Dyson, E., and Stevens, T. H. (1987) Yeast carboxypeptidase Y can be translocated and glycosylated without its amino-terminal signal sequence. *J. Cell Biol.* **104,** 1183–1191
45. Silve, S., Monod, M., Hinnen, A., and Haguenauer-Tsapis, R. (1987) The yeast acid phosphatase can enter the secretory pathway without its N-terminal signal sequence. *Mol. Cell. Biol.* **7,** 3306–3314
46. Tsai, B., Ye, Y., and Rapoport, T. A. (2002) Retro-translocation of proteins from the endoplasmic reticulum into the cytosol. *Nat. Rev. Mol. Cell Biol.* **3,** 246–255
47. Kane, R., Murtagh, J., Finlay, D., Marti, A., Jaggi, R., Blatchford, D., Wilde, C., and Martin, F. (2002) Transcription factor NFIC undergoes *N*-glycosylation during early mammary gland involution. *J. Biol. Chem.* **277,** 25893–25903
48. Lourenço, E. V., Pereira, S. R., Faça, V. M., Coelho-Castelo, A. A., Mineo, J. R., Roque-Barreira, M. C., Greene, L. J., and Panunto-Castelo, A. (2001) Toxoplasma gondii: micronemal protein MIC1 is a lactose-binding lectin. *Glycobiology* **11,** 541–547
49. Fichera, M. E., and Roos, D. S. (1997) A plastid organelle as a drug target in apicomplexan parasites. *Nature* **390,** 407–409
50. Parsons, M., Karnataki, A., Feagin, J. E., and DeRocher, A. (2007) Protein trafficking to the apicoplast: deciphering the apicomplexan solution to secondary endosymbiosis. *Eukaryot. Cell* **6,** 1081–1088
51. Robinson, S., Routledge, A., and Thomas-Oates, J. (2005) Characterization and proposed origin of mass spectrometric ions observed 30 Th above the ionised molecules of per-*O*-methylated carbohydrates. *Rapid Commun. Mass Spectrom.* **19,** 3681–3688